

Can fisheries bioenergetics modeling refine spatially-explicit assessments of climate change vulnerability?

Journal:	<i>Conservation Physiology</i>
Manuscript ID	CONPHYS-2021-106
Manuscript Type:	Research Article
Date Submitted by the Author:	07-Nov-2021
Complete List of Authors:	Troia, Matthew; The University of Texas at San Antonio, Department of Integrative Biology Perkin, Joshua; Texas A&M University, Department of Ecology and Conservation Biology
Keywords:	species distribution modeling, physiological ecology, Guadalupe bass, growth, fish, freshwater

SCHOLARONE™
Manuscripts

TITLE

Can fisheries bioenergetics modelling refine spatially-explicit assessments of climate change vulnerability?

AUTHORS

Matthew J. Troia
Department of Integrative Biology, University of Texas at San Antonio, San Antonio, TX 78249
Joshuah S. Perkin
Department of Ecology and Conservation Biology, Texas A&M University, College Station, TX 77843

CORRESPONDENCE

Matthew J. Troia
Fax: (210) 458-5005
Phone: (608) 886-6784
Email: matthew.troia@utsa.edu

LAY SUMMARY

We used bioenergetics models to project the physiological impacts of climate warming across the geographic range of Guadalupe bass, *Micropterus treculii*, and compared these projections to changes in habitat suitability from traditional species distribution models. This comparison revealed complementary insights that can inform conservation of freshwater fishes experiencing climate change.

ABSTRACT

Rising water temperature under climate change is affecting the physiology, population dynamics, and geographic distribution of freshwater taxa. We propose a novel application of individual-based bioenergetics modelling (BEM) to assess the physiological impacts of warming on freshwater fishes across broad spatial extents. We test this approach using the Guadalupe bass (*Micropterus treculii*), a species of conservation and recreational significance that is endemic to central Texas, USA. We projected historical-to-future changes (middle 20th century to end of 21st century) in daily bioenergetics of individual fish across 8,119 stream reaches and compared this output to changes in reach occupancy derived from traditional species distribution models (SDMs). SDMs project a 4.6 to 44.1% decrease in reach occupancy, depending on model parameterizations and climate change scenarios. Persistence is projected in the central Edwards Plateau region, whereas extirpations are projected for the warmer southeastern region. BEM projected a median 103.6% and 192.0% increase in somatic growth of age-1 Guadalupe bass across historically-occupied reaches under moderate and severe climate change scenarios, respectively. Higher end-of-year body size under future climate was caused by a longer growing season (mean increase of 36 and 71 days, respectively). Projected growth was geographically discordant with SDM-based habitat suitability, suggesting that SDMs do not accurately reflect fundamental thermal niche dimensions. Our assessment suggests that for locations where the species persists, Guadalupe bass may benefit from warming via increased consumption from November through March, although realized consumption gains will depend on seasonal, spatially varying changes in prey availability and other biotic and abiotic factors. More generally, we demonstrate that uniting species-specific BEMs with spatially-explicit climate change projections can elucidate the physiological impacts of climate change—including seasonal variation—on freshwater fishes across broad geographic extents to complement traditional SDMs.

INTRODUCTION

Climate change poses a significant threat to global biodiversity in the 21st century. Conservation planners need vulnerability assessments to identify and prioritize which species and regions are most in need of conservation action. Many of these assessments implement correlative species distribution models (SDMs; *sensu* Elith and Leathwick, 2009) because the input data—georeferenced occurrence records and geographic information system (GIS)-based climate layers—are profuse and easily accessible (Anderson *et al.* 2016; Fick and Hijmans, 2017). This approach facilitates the assessment of many species across broad geographic areas. For example, Crossman *et al.* (2012) used the magnitude of SDM-projected distributional shifts between historical and future climates to characterize vulnerability of 171 southern Australian plant species. In a similar study of 270 Australian Odonate dragonflies and damselflies, Bush *et al.* (2014) identified taxa that are most vulnerable to climate change, and identified priority regions for conservation actions such as regulating water extraction and protecting refugia habitats. Numerous other assessments have been performed for a variety of regions and taxa, including freshwater fishes (Radinger *et al.*, 2016; Troia *et al.*, 2019; Herrera-R *et al.*, 2020). These SDM-based assessments are invaluable to conservation planners because they incorporate many species in the assessment, are spatially contiguous, and span broad geographic extents.

A limitation of SDM-based assessments is that they do not explicitly assess physiological impacts of climate change. This can lead to uncertain and inaccurate vulnerability assessments because the realized climatic niche in the present may not reflect the fundamental climatic niche (Kearney and Porter, 2009; Sax *et al.*, 2013). Recent assessments are beginning to estimate the physiological impacts of climate change across broad spatial extents. For example, Comte and Olden (2017) used laboratory-derived upper thermal tolerances of fishes and global temperature projections to assess global patterns of vulnerability among freshwater and marine fishes. This assessment revealed high warming exposure for temperate freshwater faunas versus high

1
2
3 physiological sensitivity for temperate marine faunas. Similarly, Dillon *et al.* (2010) found that
4 metabolic sensitivity of terrestrial ectotherms is higher for tropical taxa compared with temperate
5 and polar taxa, suggesting that physiological impacts of climate warming will be greater in the
6 tropics despite relatively moderate rates of warming. These physiology-based assessments are
7 important because they can reveal causal links between specific climatic conditions and the
8 performance of individuals and populations. For example, Briscoe *et al.* (2016) showed that timing
9 of rainfall events relative to extreme heat events limit survival of koalas at their contemporary
10 range edges and will likely drive shifts in these range edges under future climate.
11
12

13
14
15
16
17
18
19
20
21
22
23
24
25
26
27
28
29
30
31
32
33
34
35
36
37
38
39
40
41
42
43
44
45
46
47
48
49
50
51
52
53
54
55
56
57
58
59
60
Freshwater fishes are diverse, imperiled, and in need of vulnerability assessments and
conservation action (Strayer and Dudgeon, 2010; Vörösmarty *et al.*, 2010). Bioenergetics models
(hereafter 'BEM') have been used in fisheries science since the 1970s to inform the management of
recreational and commercial fish stocks (Deslauriers *et al.*, 2017). The approach uses a species-
specific energy balance equation to estimate energy gains—via consumption of prey—and energy
losses—via metabolism, egestion, and excretion—to estimate daily energy budgets of individuals.
These energy balance equations are based on intrinsic physiological and behavioral traits of the
species and on extrinsic environmental conditions. Prolonged periods of bioenergetic deficits lead
to mortality, whereas bioenergetic surpluses are directed toward somatic growth and reproduction
(Garvey *et al.*, 2004; Lawrence *et al.*, 2015). BEM provide a physiology-based approach to assess
climate change vulnerability of fishes that go beyond assessments based on physiological thermal
limits (*e.g.*, Deutsch *et al.*, 2008; Feeley and Silman, 2010; Comte and Olden, 2017). Pease and
Paukert (2014) used BEMs to estimate prey consumption and growth potentials for four
populations of smallmouth bass (*Micropterus dolomieu*) under historical and future thermal
regimes. Nevertheless, there are few such applications of BEM. It is surprising that BEM have not
been used for broader-scale climate change vulnerability assessments given (1) the accumulation of
species for which BEM are parameterized (*i.e.*, at least 70 species; Deslauriers *et al.*, 2017); (2) the

accessibility of GIS data layers describing environmental conditions in freshwater habitats (Hill *et al.* 2016); and (3) conceptual development of BEM for conservation of rare species (Petersen *et al.* 2008).

Here, we present an assessment of climate change vulnerability for the Guadalupe bass (*Micropterus treculii*)—a fish endemic to the Edwards Plateau region of central Texas, USA (Figure 1A). The small geographic range—only 20,000 to 200,000 km² (NatureServe, 2010)—and the ongoing threat of hybridization with non-native smallmouth bass (*M. dolomieu*; Bean *et al.*, 2013) make Guadalupe bass a species of conservation concern (Hubbs *et al.*, 2008). Guadalupe bass are also popular among recreational anglers, meaning the persistence of robust populations is of cultural and economic importance for the region (Thomas, 2015). Still, vulnerability of Guadalupe bass to 21st century climate change remains unknown. To assess climate change vulnerability, we used BEM to project changes in bioenergetic budgets of individuals and correlative SDMs to project changes in reach occupancy under historical and end of 21st century climate scenarios. Because BEM parameters do not yet exist for Guadalupe bass, we compiled parameters of largemouth bass (*Micropterus salmoides*) and used a novel parameter resampling algorithm to develop and validate an ensemble of BEM. SDMs were parameterized with open-source occurrence records, and landscape and climatic covariates using the Maximum Entropy algorithm (Phillips *et al.*, 2004; Vollerling *et al.*, 2019). Both models were projected to 8,119 confluence-to-confluence stream reaches within the Guadalupe bass range. By comparing occurrence-based and physiology-based approaches using this broad-scale, spatially-explicit framework of species distribution modelling, we provide novel insight into how climate change will (1) affect multiple levels of the biological hierarchy and (2) across Guadalupe bass geographic range where vulnerability (or benefits) will be greatest. Implementing BEM on a daily time step also reveals seasonal variation in bioenergetic budgets, providing insight into another dimension of vulnerability—phenological changes in physiological performance.

MATERIALS AND METHODS

Study system

The Guadalupe bass is native to the Brazos, Colorado, Guadalupe, and San Antonio river basins and has been introduced to the Nueces river basin of Texas, USA (Figure 1A). Streams of these basins flow generally from northwest to southeast. Most of these basins drain the high plains in the west, Edwards Plateau in the center, and the coastal plain in the east. Precipitation declines markedly from 1360 mm per year in the east to 345 mm per year in the west and mean annual air temperature ranges from 13.5°C in the northwest to 22.1°C in the south. We implemented SDMs and BEM for all perennial, confluence-to-confluence stream reaches (hereafter 'reaches') within the five basins. We acquired reaches from the National Stream Internet flowline layer (Nagel *et al.*, 2017) and retained perennial reaches (NHD FCode = 46006), yielding 8,119 reaches.

Species distribution modelling

We used SDM to map the habitat suitability of Guadalupe bass to all 8,119 reaches in the study region. We extracted records of Guadalupe bass occurrence ($n=240$) between 1950 and 1980 from the IchthyMaps dataset (Frimpong *et al.*, 2016) (Figure 1A). We acquired GIS-derived predictor variables describing hydrographic, geological, and soil characteristics (hereafter 'landscape' variables) for the 8,119 reaches from the StreamCat dataset (Hill *et al.*, 2016). We acquired averages of monthly precipitation totals and monthly air temperature minima, means, and maxima (hereafter 'climate' variables) for all reaches between 1960 and 1990 using the ClimateNA program (Wang *et al.*, 2016). Although air temperature and precipitation are not direct measures of parallel in-stream conditions (water temperature and flow, respectively), these climatic conditions are effective surrogate covariates for modelling habitat suitabilities of stream-dwelling fishes (McGarvey *et al.*, 2018). We checked variable pairs for correlations (Pearson's r) and retained only uncorrelated variables ($|r| \leq 0.7$) known to affect in-stream habitat suitability of stream fishes (Huang and Frimpong, 2015) (Supplementary Table 1).

We fit SDMs with the Maximum Entropy algorithm using the MIAMaxent library in R (Vollering *et al.*, 2019). This model was used to project habitat suitability to all 8,119 reaches under seven different projections, each representing a different combination of climate scenarios (Table 1). For projections to future climates (projections 2-7), we used scenarios of moderate (Representative Concentration Pathway; hereafter ‘RCP 4.5’) and high (RCP 8.5) greenhouse gas emissions derived from an ensemble of 15 general circulation models (Wang *et al.*, 2016). Because we were interested in exploring effects of temperature and precipitation changes independently of one another—and comparing temperature-only effects to BEM projections—we performed projections in which both temperature and precipitation change (projections 2 and 6), only temperature changes (3 and 7), or only precipitation changes (4 and 8). We used the probability ratio output as habitat suitability and interpreted reaches with values ≥ 1 as being occupied following Vollering *et al.* (2019). We defined four historical to future projection states: persist (occupied to occupied), colonize (unoccupied to occupied), extirpate (occupied to unoccupied), unoccupied (unoccupied to unoccupied). Our definition of ‘occupied’ is based strictly on habitat suitability of the reach and does not account for dispersal limitation, particularly as it relates to the ‘colonize’ state.

We evaluated model performance by splitting records into a 50% training set ($n = 120$), fitting the model, and computing the area under the curve (AUC) of the receiver operator characteristic on the remaining records (testing set; $n = 120$ records). Because the IchthyMaps dataset does not include putative absence records, we selected a random sample (equal to the number of records in the testing set; $n=120$) of reaches in which a congener (*Micropterus spp.*) was present in the IchthyMaps dataset and Guadalupe bass was not present. This method increases the likelihood of selecting true absences because many records included in the IchthyMaps dataset originate from whole-community fish surveys (Mateo *et al.*, 2010; Huang and Frimpong, 2015). This independent cross-validation procedure was repeated ten times, each time selecting different

subsets of records for training and testing. The mean AUC of these ten repetitions was computed and used to evaluate model performance. We evaluated variable performance by removing each variable, in turn, and computing the percent reduction in AUC relative to the model with all variables. To evaluate the predictive capability of landscape versus climate variables, we evaluated model performance of models fit with (1) landscape and climate variables, (2) landscape variables only, and (3) climate variables only.

Bioenergetics modelling – model descriptions

We used BEM to map somatic growth potential (hereafter ‘growth’) of Guadalupe bass to all 8,119 reaches in the study region. The bioenergetics model took the form of the following equation, after Hanson *et al.* (1997):

$$G = C - (R + SDA + E + U) \quad \text{Equation 1}$$

where G is mass gained via growth, C is mass gained via consumption, R is mass lost via respiration, SDA is mass lost via specific dynamic action (the energetic cost of digestion), E is mass lost via egestion, and U is mass lost via excretion. Mass dependence of respiration and consumption are modelled as power functions of the form:

$$R = R_A \times M^{R_B} \quad \text{Equation 2}$$

$$C = C_A \times M^{C_B} \quad \text{Equation 3}$$

where R and C are mass-specific routine metabolism measured in grams of O_2 consumed per gram of body mass and maximum consumption as grams of prey consumed per gram of body mass, respectively, M is mass, R_A and C_A are slopes and R_B and C_B are y -intercepts. We converted O_2 consumption to joules using the oxycalorific coefficient, 13,560 J/g O_2 (Hanson *et al.*, 1997) and grams of prey consumed to joules using the median energy density reported for larval fish, the presumed prey of age-1 Guadalupe bass (3,698 J/g wet mass; Henderson and Ward, 1978). The temperature dependence equation for respiration follows the exponential form presented by Hanson *et al.* (1997) (Equation 4):

$$R = e^{R_Q \times T}$$
Equation 4

where R is mass-specific routine respiration, R_Q is the slope of the respiration function at low water temperatures, and T is temperature. The temperature dependence equation for consumption follows the monotonic form presented by Hanson *et al.* (1997) after Kitchell *et al.* (1977) (Equation 6):

$$C = V^X \times e^{(X \times (1 - V))}$$
Equation 5

where:

$$V = (CTM - T)/(CTM - CTO)$$
$$X = (Z^2 \times (1 + (1 + 40/y)^{0.5})^2)/400$$
$$Z = \ln(C_Q) \times (CTM - CTO)$$
$$Y = \ln(C_Q(CTM - CTO + 2))$$

where C is mass-specific respiration, CTM is the temperature above which feeding ceases, CTO is laboratory temperature preferendum, and C_Q approximates a Q_{10} (*i.e.*, the rate at which consumption increases at low temperature). We assumed egestion and excretion to be constant proportions of consumption, and specific dynamic action to be a constant proportion of respiration (Hanson *et al.* 1997). BEM also require inputs of the proportion of maximum consumption at which an individual feeds (C_p) and the activity multiplier of respiration (R_{ACT}) which takes into account the metabolic costs of activity beyond routine metabolic rate (*e.g.*, active swimming against streamflow, pursuing mobile prey).

Because laboratory measurements of the mass-dependence and temperature-dependence of consumption and respiration have not been published for Guadalupe bass (Deslauriers *et al.*, 2017), we borrowed these laboratory-derived BEM parameters from largemouth bass (Supplementary Table 2). Largemouth bass is the most recent common ancestor of Guadalupe bass, having diverged approximately 5.2 million years ago (Near *et al.*, 2003), and occupies a climatic envelope that contains Guadalupe bass (NatureServe, 2010). As such, largemouth bass is the best

surrogate species currently available for modelling bioenergetics budgets of Guadalupe bass (Petersen *et al.*, 2008). Mass-dependent respiration and consumption were modelled as exponential functions (Equations 2 and 3). Temperature-dependent respiration was modelled as an exponential function (Equation 4) and temperature-dependent consumption was modelled as a monotonic function (Equation 5). Because it is unlikely that BEM parameters of Guadalupe bass are precisely equivalent to largemouth bass, we performed a parameter resampling procedure to generate additional parameter sets (hereafter 'synthetic parameter sets'). For each parameter, we sampled from a uniform distribution bounded by a minimum value 5% lower than the largemouth bass parameter value and a maximum value 5% larger than the largemouth bass parameter value. These bounds generated parameter values that are within the range of parameter values observed for other fish species (Deslauriers *et al.*, 2017), and therefore are biologically realistic. We used this procedure to generate 50 synthetic parameter sets.

Bioenergetics modelling – validation

We validated BEM using empirical growth of a Guadalupe bass population in the South Llano River. We estimated age-specific growth using back-calculated length-at-age measurements of scales taken from fish age-1 fish spawned between 2005 and 2011 (Groeschel-Taylor *et al.*, 2019). Lengths-at-age were converted to masses-at age using von Bertalanffy equations of Guadalupe bass (Groeschel-Taylor *et al.*, 2019). We used BEM to project growth beginning on Julian day 1 and ending on Julian day 365. These projections require two inputs: (1) initial fish mass, and (2) mean daily water temperature during the projection period. Fish mass was assumed to be 6.4g for age-1 fish (Groeschel-Taylor *et al.*, 2019). We estimated mean daily water temperatures for all 17 reaches within the South Llano River study area of Groeschel-Taylor *et al.* (2019) using a two-step approach. First, we acquired monthly mean air temperatures at each reach from the ClimateNA program (Wang *et al.*, 2016) for the years during which growth was measured (2005 through 2011). We converted air temperature to water temperature using sigmodal air-water temperature

relationships derived by Punzet *et al.* (2012) for the warm-temperate Köppen–Geiger climate zone. Second, we fit a sine function to the annual temperature cycle at each reach, separately, using the monthly water temperatures and assuming these monthly values correspond to the middle day of each month (*i.e.*, Julian days 15, 46, 74, 105, 135, 166, 196, 227, 258, 288, 319, and 349). We then used these sine functions to interpolate water temperature to all 365 Julian days at the 17 reaches.

We simulated growth for age-1 individuals using each of the 50 synthetic parameter sets, assuming metabolic costs of activity were 100% ($R_{ACT} = 1.0$) and prey consumption was 44%, 47%, 50%, 56%, or 56% of maximum capacity ($C_p = 0.44, 0.47, 0.50, 0.53, \text{ or } 0.56$). We also simulated growth under the assumption of elevated metabolic costs (150%, $R_{ACT} = 1.5$) and prey consumption of 61%, 64%, 67%, 70%, or 73% of maximum capacity ($C_p = 0.61, 0.64, 0.67, 0.70, \text{ or } 0.73$). We derived these ranges of C_p values by setting start mass and end mass of age-1 Guadalupe bass and solving the largemouth bass BEM of Rice *et al.* (1983) for C_p under baseline ($R_{ACT} = 1.0$) and elevated ($R_{ACT} = 1.5$) metabolic demand. We then used these approximated C_p values as midpoints (0.50 for $R_{ACT} = 1.0$, 0.67 for $R_{ACT} = 1.5$) and added two lower (−4% and −2%) and two upper (+2% and +4%) scenarios. Of the 500 simulations (50 synthetic parameter sets x 5 C_p scenarios x 2 R_{ACT} scenarios), we identified those that projected end-of-growing-season simulated length within $\pm 2.5\%$ of end-of-year empirical length, and retained these BEM for the climate change vulnerability assessment described below. We used simulated length at the end-of-growing-season (*i.e.*, last Julian day with a daily bioenergetics surplus) because mass declines during the remaining days of the calendar year whereas length does not. Hence, using simulated end-of-year mass and converting it to length would underestimate actual length gained during the calendar year.

Bioenergetics modelling – projecting bioenergetics to reaches

We used BEM to project growth of age-1 Guadalupe bass for all 8,119 reaches assuming climate under the historical time period and the two future time periods (RCP 4.5 and RCP 8.5). We assumed fish mass was 6.4 g on Julian day 1, and projected growth through Julian day 365. We

estimated mean daily water temperatures for all 8,119 reaches using the same two-step approach described above. We used these simulated growth trajectories to estimate end-of-year mass. We also used daily bioenergetics budgets to explore the duration of growing season, which we defined as the number of consecutive days of bioenergetics surplus. All BEM were developed and projected using original scripts in R.

Statistical analyses

We used generalized additive models to evaluate the spatial (*i.e.*, among reaches) concordance between BEM and SDM projections. We fit three sets of models to test three statistical hypotheses: (1) historical end-of year body size is positively correlated with historical habitat suitability (Hypothesis 1); (2) historical end-of year body size is positively correlated with change in habitat suitability between historical and future time periods (Hypothesis 2); and (3) change in end-of-year body size between historical and future time periods is positively correlated with change in habitat suitability between historical and future time periods (Hypothesis 3). Confirmation of hypothesis 1 would support the biological hypothesis that low habitat suitability limits growth capacity at range margins, whereas high habitat suitability facilitates greater growth capacity within the core of the range. Confirmation of hypothesis 2 would support the biological hypothesis that historical habitat suitability will maintain conditions suitable for growth capacity in the future. Confirmation of hypothesis 3 would support the biological hypothesis that historical to future reduction in growth capacity will be caused by the reduction in habitat suitability, whereas increased habitat suitability will facilitate increased growth capacity. Alternatively, no relationship or a negative relationship would indicate that historical spatial variation in habitat suitability or historical to future change in habitat suitability is associated with other aspects of individual performance (*e.g.*, reproduction, recruitment, etc.).

For both sets models, SDM-based habitat suitability [*i.e.*, $\log_2(\text{PRO}+1)$] was the predictor variable and BEM-based growth was the response variable. Both model sets also included

alternative models with ecoregion fit as a factor because inspection of mapped projections revealed regional differences in BEM and SDM outputs (Supplementary Figure 1). Models were fit using restricted maximum likelihood in the mgcv library in R (Wood and Scheipl, 2014). Model significance was assessed using an *F*-test at $P < 0.05$ and performance was assessed using deviance explained.

RESULTS

Species distribution models

SDMs performed moderately well when fit with landscape variables only (mean AUC = 0.78) or with landscape variables and climate variables (0.79), but poorly when only climate variables were used (0.68). The most important predictor variable was baseflow index (percent change in AUC = -2.01%), followed by January minimum temperature (-1.13%), and soil erodibility factor (-1.09%) (Supplementary Table 1). SDMs projected the highest historical habitat suitability within the Edwards Plateau, particularly those within the Guadalupe River basin, as well as the mainstem Guadalupe and San Marcos Rivers to the southeast of the Edwards Plateau (Figure 1B). Projected reach occupancy under historical climate was 2,871 reaches, constituting 35.4% of the 8,119 perennial reaches within the five-basin range of Guadalupe bass. Occupancy is projected to decrease (-4.6 to -44.1%) between the historical and future time periods (Table 1). SDM projections that assume only temperature changes (Projections 2, 3, 5 and 6) project more reach extirpations (-26.0% to -44.1%) than projections that assume only precipitation changes (Projections 4 and 7; -4.6% to -7.6%), suggesting that historical distributions are limited more by temperature than by precipitation. Extirpations are projected for reaches to the south and east of the Edwards Plateau, whereas relatively few colonizations (Table 1) are projected for reaches to the north of the Edwards Plateau (Figure 1C-D). This spatial pattern of occupancy transition is similar for projections that assume only temperature changes (Supplementary Figure 1). For projections

assuming only precipitation changes, extirpations are limited to reaches in the arid southwestern region (Supplementary Figure 1).

Bioenergetics models

The 500 simulated parameter sets projected a wide range of growth trajectories for age-1 Guadalupe bass; however, 36 simulations projected end-of-growing-season simulated length within $\pm 2.5\%$ of end-of-year empirical length in the South Llano River validation reaches (Figure 2, Supplementary Table 2, Supplementary Figure 5). We focused on these 36 simulations for BEM spatial interpretation. Projected end-of-year mass for age-1 fish under historical climate across 2,871 historically-occupied reaches was median 22.5 g (range: 12.7 g to 51.6 g). Under future climate, projected end-of-year mass increased to median 45.1 g (range: 27.0 g to 89.4 g) for the RCP 4.5 scenario and increased to median 64.3 g (range: 37.5 g to 119.9 g) for the RCP 8.5 scenario. Across the 8,119 perennial reaches, end-of-year masses were highest in the south and lowest in the north (Figure 3A). Coefficients of variation across the 36 different simulations ranged from 6% to 72%, with greater uncertainty (higher CVs) in the north where projected end-of-year mass was lowest (Figure 3B). Future changes in end-of-year mass were projected to be proportionally higher for reaches in the north and on the Edwards Plateau (Figure 3C-D). These reaches with higher future growth were in regions of historically lower temperatures that are projected to warm at a faster rate than regions with historically higher temperatures (Supplementary Figure 2), owing to the sigmoidal shape of the Punzet *et al.* (2012) air-water temperature model (Supplementary Figure 3).

Daily bioenergetic deficits were projected during the cold season and bioenergetic surpluses during the warm season under historical climate (Figure 4A), resulting in a growing season duration of 203 days (median across 2,871 historically-occupied reaches; range: 190 days to 237 days). Growing seasons were projected to increase to 239 (range: 225 days to 290 days) under the future RCP 4.5 scenario and 274 days (range: 253 days to 345 days) under the future RCP 8.5

scenario (Figure 4B-C). Mass accumulated during the growing season under historical climate (Figure 4D). The rate of mass accumulation was higher under future climate, resulting in larger end-of-year body size (Figure 4E-F).

Congruence between bioenergetics models and species distribution models

End-of-year mass and habitat suitability during the historical time period were significantly correlated, but the relationship was weak and not monotonic (estimated $df = 8.599$, reference $df = 8.957$, $F = 24.27$, $P < 0.01$, deviance explained = 3.01%; Figure 5A). Including ecoregion as a factor increased deviance explained for the model (estimated $df = 7.953$, reference $df = 8.727$, $F = 10.47$, $P < 0.01$, deviance explained = 63.3%; Figure 5B). For the Edwards Plateau, end-of-year mass and habitat suitability were positively correlated (Figure 5B, green line). Thus, Hypothesis 1—historical end-of year body size is positively correlated with historical habitat suitability—was not supported.

Historical to future change in end-of-year mass and historical habitat suitability were significantly correlated, but the relationship was weak and not monotonic (estimated $df = 8.496$, reference $df = 8.932$, $F = 66.69$, $P < 0.01$, deviance explained = 7.55%; Figure 6A). Including ecoregion as a factor increased deviance explained for the model (estimated $df = 8.67$, reference $df = 8.970$, $F = 29.72$, $P < 0.01$, deviance explained = 31.6%; Figure 6C). For the Edwards Plateau, change in end-of-year mass and historical habitat suitability were negatively correlated (Figure 6C, green line). Thus, Hypothesis 2—historical end-of year body size is positively correlated with change in habitat suitability between historical and future time periods—was not supported.

Historical to future change in end-of-year mass and historical to future change in habitat suitability were significantly and positively correlated, indicating concordance between BEM and SDM projections (estimated $df = 8.771$, reference $df = 8.984$, $F = 363.8$, $P < 0.01$, deviance explained = 30.8%; Figure 6B). Including ecoregion as a factor increased deviance explained for the model

(estimated $df = 8.632$, reference $df = 8.960$, $F = 253.8$, $P < 0.01$, deviance explained = 45.8%; Figure 6D). The relationship remained positive for the Edwards Plateau and High Plains (Figure 6D, green and blue lines), but not for the Coastal Plain (Figure 6D, red line). Thus, Hypothesis 3— change in end-of-year body size between historical and future time periods is positively correlated with change in habitat suitability between historical and future time periods—was supported.

DISCUSSION

Historical distribution, ecology, and physiology

A fundamental goal of ecology and an objective of this study was to elucidate drivers of geographic range limits. Geographic range limits are driven by a combination of abiotic, biotic, historical, and spatial processes (Holt *et al.*, 2005; Soberón, 2009). These general processes also constrain distributions of freshwater fishes, whereby drainage divides, climate, landscape geology, in-stream habitat, and species interactions constrain distribution and abundance of species at broad spatial extents (Tonn *et al.*, 1990; Jackson *et al.*, 2001). Field studies of distribution and habitat use support this paradigm for Guadalupe bass, which associates with spring fed streams of the Edwards Plateau (Edwards, 1980; Perkin *et al.*, 2010) and ostensibly is geographically restricted by contemporary drainage divides of the western gulf coast (Near *et al.*, 2003; Hoagstrom *et al.*, 2011). Our SDM projections of historical habitat suitability confirmed the spatial association with the Edwards Plateau and the high predictive capability of baseflow index in these models confirmed the association with spring-fed streams (Curtis *et al.*, 2015). Minimum January temperature also was an important predictor of historical distribution, suggesting that cold winter temperatures preclude persistence in the northwestern unoccupied reaches of the Colorado and Brazos River basins. The BEM simulations under historical climate consistently projected energy deficits during the winter months and these deficits are of greater magnitude and persist for a longer duration of the cold season in the north compared to the south. These physiological projections thus support the hypothesis that cold winter temperature could limit the northern

range edge of Guadalupe bass and reveals a potential mechanism of winter starvation. BEM-based studies of largemouth bass have shown that cold temperatures and short growing seasons cause starvation of juveniles and drive the cold range edge throughout North America (Garvey *et al.*, 1998; Fullerton *et al.*, 2000). A second (and not necessarily mutually exclusive) interpretation of high predictive capability of minimum January temperature from our SDMs is that *warm* winter temperatures preclude persistence in the southeastern unoccupied reaches along the gulf coastal plain. SDMs fitted with temperature predictors projected future erosion of habitat suitability along the southeastern range margin relative to models fitted without temperature predictors (Supplementary Figure 2), supporting the interpretation that winter temperature drives the warm range edge. Whether winter temperature actually constrains the warm-edge limit of Guadalupe bass seems dubious, given that most studies invoke intolerance to low temperature as a constrainer of cold-edge limits among ectotherms generally (Sunday *et al.*, 2012) and fishes specifically (Wood *et al.*, 2020). Nevertheless, one potential mechanism is that a cold winter—and subsequent warming in the spring—is a required seasonal cue for reproduction for Guadalupe bass as it is for other temperate freshwater fishes (Shuter *et al.*, 2012). Our BEMs revealed explicit insight into growth and implicit insight into recruitment (*e.g.*, size dependent winter survival; *sensu* Fullerton *et al.*, 2000); however, additional lines of inquiry will be needed to evaluate reproduction, generally, and the seasonal cue hypothesis, specifically (Firkus *et al.*, 2018; Heins, 2020). A third interpretation is that our SDMs revealed a spurious correlation between winter temperature and other important predictors—a common issue with correlative SDMs when inferring causality (Kearney and Porter, 2009). In Texas, winter and summer temperatures are not strongly correlated (Pearson $r = -0.25$), meaning that high summer temperature (a poor predictor; Supplementary Table 1) as a driver of warm-edge limits can be ruled out. From a physiological perspective, laboratory growth of Guadalupe bass indicates high optimal temperature for growth (27°C; Sullivan *et al.* 2013) relative to historical summer temperatures along the southeastern range edge

($<28.5^{\circ}\text{C}$; Supplementary Figure 3). Thus, it is unlikely that southern range limits are driven by sensitivity of Guadalupe bass to high summer temperatures. The northwest-to-southeast winter temperature gradient spatially correlates with the transition from Edwards Plateau to Coastal Plain and an accompanying suite of geological and biological changes (Hoeinghaus *et al.*, 2007). It is likely that some combination of spuriously correlated geological and biological conditions limit Guadalupe bass populations in the Coastal Plain.

Precipitation did not provide strong predictive capability in our SDMs. This is further supported by the SDM projections under future climate scenarios that revealed similar extirpation and colonization patterns whether precipitation variables were included or not. This finding is surprising given the strong east-to-west precipitation gradient spanning the historical range of Guadalupe bass. Western range limits of Guadalupe bass are almost certainly driven by the east-to-west transition of perennial to intermittent flow regime (Muneepeerakul *et al.*, 2008; Perkin *et al.*, 2015), although our SDMs did not include explicit predictors representing flow regime. While other SDM-based studies have shown that precipitation variables can be useful surrogates of instream flow conditions (McGarvey *et al.*, 2018), this may not apply to all regions particularly where precipitation gradients span transitions from perennial to intermittent (or ephemeral) streamflow like in Texas. Another potential explanation for poor predictive capacity of precipitation variables is that we included baseflow index—an effective surrogate for perennial flow—in our SDMs and this variable was highly predictive. The interaction between precipitation, baseflow index, and the realized streamflow regime is not of the highest importance for characterizing historical range limits, but will be very important when making projections about novel future climate, flow, and Guadalupe bass population viability (Jiménez-Valverde *et al.*, 2009; Birdsong *et al.*, 2015).

Competition with a more widespread congener and/or an interaction milieu associated with adjacent high-richness assemblages often limit ranges of endemic species (Graham *et al.*, 2010; Jankowski *et al.*, 2010). We did not explicitly incorporate biotic factors into our SDMs or BEMs,

although prey availability and/or interspecific competition may be important drivers of Guadalupe bass range limits, as they are in other freshwater fishes (Taniguchi and Nakano, 2000; Finstad *et al.*, 2011). The eastern range limit of Guadalupe bass corresponds with a rapid increase in fish species richness (Hubbs *et al.*, 2008; Muneepeerakul *et al.*, 2008), which may intensify competition and reduce realized consumption (*i.e.*, reduce the value of the *CP* parameter in our BEMs). Prey production likely also decreases along southeast-to-northwest climatic gradients (Patrick *et al.*, 2019), and similarly may reduce realized consumption of Guadalupe bass along the northern and western range limit. Although we did not extrapolate SDMs or BEMs beyond drainage basins in which Guadalupe bass historically have occurred, it is likely that BEMs (and to a lesser extent SDMs) would identify suitable habitat in drainages to the east where thermal regimes are similar (*e.g.*, Trinity and Sabine River basins).

We conclude that historical range limits of Guadalupe bass are driven by multiple factors and that SDMs and BEMs offer different yet informative insights into these drivers. Further refinement of both modelling approaches—particularly the incorporation of (1) proximal abiotic factors (*e.g.*, flow intermittency) and (2) biotic factors (*e.g.*, prey density)—will improve understanding of Guadalupe bass distribution and abundance. Finally, integration with additional modelling approaches that can incorporate spatial variation in reproduction will also improve understanding of range edge dynamics of Guadalupe bass.

Climate change impacts

A primary objective of this study was to assess vulnerability of Guadalupe bass to climate change. Our SDM-based and physiology-based assessments yielded different answers—SDMs forecasted a decline in habitat suitability, whereas BEMs forecasted an increase in growth capacity. Nevertheless, the alternative approaches yielded complementary insights into the spatial distribution of vulnerability, and potential mechanisms contributing to vulnerability. Climate envelope approaches (*i.e.*, correlative SDMs; *sensu* Elith and Leathwick, 2009) often forecast

geographic range shifts toward colder and wetter regions (Ackerly *et al.*, 2010; Comte and Grenouillet, 2013). Our SDMs matched this expected response to temperature—habitat suitability erodes at the warm-range edge in the southeastern Coastal Plain. The key environmental variable driving this forecasted erosion—minimum winter temperature—however, is an unlikely driver of warm-range edge retraction (Sunday *et al.*, 2012). Our BEMs, on the other hand, projected an increase in growth potential throughout the historical range, including along the southeastern Coastal Plain. Other physiology-based forecasts indicate similar responses in growth potential for temperate freshwater fishes (Pease and Paukert, 2014; Hartman, 2017) and other temperate ectothermic taxa (Deutsch *et al.* 2008) under climate change. This increased growth potential is feasible, given that future water temperatures are not forecasted to exceed optimal temperature for growth (27°C; Sullivan *et al.*, 2013). However, growth potential would have to be matched by increased prey availability and while not being impeded by stronger competition with existing competitors and/or novel competition in reassembled communities (Urban *et al.* 2012).

On the northern range edge, SDMs projected modest increases habitat suitability that—assuming dispersal opportunities exist—could facilitate colonization of some historically unoccupied reaches in the Colorado and Brazos River basins. BEMs also forecast the highest historical-to-future increase in growth potential in the northwest (as well as in the southwestern portion of the Edwards Plateau). This is caused by the WT model projecting the greatest increase in WT in regions with 10-20°C air temperatures (due to sigmoidal air-water relationship; Supplementary Figure 4; Punzet *et al.*, 2012). This artifact of our simplistic air-water temperature model highlights the importance of improved understanding and forecasting of stream temperatures under anticipated changes in air temperature and surface-groundwater interactions (Caldwell *et al.*, 2020).

Surprisingly, our SDMs did not forecast an eastward shift in habitat suitability away from the dry west and toward the wet east. This is likely the result of a breakdown in the causal links

between precipitation, in-stream flow conditions, and Guadalupe bass occupancy. Indeed, the density of perennial streams on which Guadalupe bass rely are forecasted to decline across historical Guadalupe bass range, particularly in the arid western portions of the Colorado and Brazos River basins (Smith *et al.*, 2013). Thus, it is likely that Guadalupe bass populations on the western range edge will be lost as their habitats transition from perennial to intermittent (Perkin *et al.*, 2015). Given the contribution of the Edwards-Trinity Aquifer to surface flow of perennial streams, the extent and magnitude of dewatering will depend on amplifying interactions between climate change (*i.e.*, as we have projected) and groundwater extraction (*i.e.*, not explicitly included in our SDMs). We did not project habitat suitability or growth potential in the basins to the east of the Brazos River basin (*i.e.*, Trinity and Sabine River basins) because there are no natural dispersal opportunities. Whether habitat suitability and/or growth potential would increase in these adjacent basins under future climate would likely depend on in-stream conditions (*e.g.*, proximal correlates of baseflow index).

Another objective of our BEM assessment was to evaluate seasonal changes in Guadalupe bass growth caused by warming in the 21st century. Our BEMs indicate an energy deficit during the cold season when metabolic costs exceed consumptive gains. Warmer year-round temperatures throughout Guadalupe bass range under future climate therefore are projected to advance the onset of feeding in the spring and extend feeding in the autumn, yielding a longer growing season and larger end-of-year body size. Under historical temperature regimes, Guadalupe bass are projected to maintain positive growth even in the hottest period of summer because consumptive gains can exceed metabolic losses. Future projections, particularly the RCP 8.5 scenario, metabolic costs are projected to approach or even exceed consumptive gains for several of the parameter sets meaning that growth could be suppressed both in winter and mid-summer. These changes in seasonal energy budgets will likely affect allocation of energy to somatic growth versus reproduction and subsequent population dynamics.

Broader implications

Mechanistic niche modelling was formalized by Kearney and Porter (2009), and has informed basic research aimed at understanding the ecological processes driving species distributions as well as applied research aimed at forecasting species vulnerability to anthropogenic environmental change (*e.g.*, Briscoe *et al.*, 2016). Nevertheless, implementation has focused largely on terrestrial insects (*e.g.*, Buckley *et al.*, 2011), amphibians (*e.g.*, Kearney *et al.*, 2008), and reptiles (*e.g.*, Buckley, 2008). The BEM approach used by fisheries professionals conceptually aligns with mechanistic niche modelling (*sensu* Kearney and Porter, 2009), but to date is not implemented at fine spatial resolutions (*i.e.*, individual stream reaches) while spanning broad spatial extents (*i.e.*, 1000s of reaches). Our study demonstrates that this novel application of BEM is generalizable to any region or fish species. Nevertheless, several challenges currently preclude broader implementation of BEMs as tools to forecast climate change vulnerability of fishes in a spatially explicit manner.

First, a challenge of developing physiology-based conservation assessments is that physiological traits of species in need of conservation are often poorly known. For example, 39% of the 700-plus species of North American freshwater fishes are imperiled (Jelks *et al.*, 2008), yet bioenergetics models have been parameterized for only 73 fish species worldwide (Deslauriers *et al.*, 2017), few of which are among the 270-plus imperiled species in North America. In the near term, the parameter resampling approach we used (*sensu* Petersen *et al.*, 2008)—combined with validation from field growth studies—represents an effective strategy for rapid development of BEMs for numerous imperiled species. Indeed, data on field growth are generally available and have recently been compiled and synthesized for broad-scale meta-analyses (*e.g.*, Rypel, 2014). In the long term, physiological reaction norms for functionally- and phylogenetically-underrepresented taxa should be accumulated (Chown and Gaston, 2016). Second, high spatiotemporal resolution temperature data for freshwater habitats is needed. Indeed, poorly known air-water temperature

relationships and the influence of surface-groundwater interactions contributed to uncertainty in our BEM projections. Current open-source datasets tend to be spatially comprehensive, often spanning tens of thousands of confluence-to-confluence reaches, but lack daily temporal resolution needed for BEM (NorWeST; Isaak *et al.*, 2017). It is likely that spatiotemporally comprehensive data will become available in the near future (*e.g.*, Hydroclim; hydroclim.org) as the open-source data culture grows (McManamay and Utz, 2014). Third, spatiotemporally comprehensive biological information is needed to better understand how predator-prey interactions (*i.e.*, spatiotemporal variation in CP parameter) and behavior (*i.e.*, spatiotemporal variation in ACT parameter) vary along environmental gradients. Surrogates of these factors can be acquired from existing geospatial datasets (*e.g.*, net primary production; Deines *et al.*, 2015) or statistical models (*e.g.*, secondary production; Patrick *et al.*, 2019). This information will facilitate the adjustment of CP and ACT parameters in BEMs to more realistically project energy budgets of fish.

Conclusions

Our work demonstrates the utility of applying an ensemble of approaches to assess ecological responses to future climate change (Hollowed *et al.*, 2013). Comparison between habitat suitability based on ENM and growth capacity based on BEM indicated no spatial concordance between the two approaches, whereas comparison between historical to future change in these responses revealed spatial concordance between the two approaches. The emergent pattern is that habitat suitability may or may not correlate with potential for end-of-year mass, perhaps because increases in temperature are interpreted differently within each modelling approaches. In the BEM approach, warmer temperatures that do not exceed critical thermal maxima result in greater gain in mass (assuming unlimited resources for growth); whereas, in the ENM approach, correlative temperature relationships equate to occurrence based on unknown and unmeasured mechanisms. It is possible that unmet increases in energetic demand under greater temperatures is a mechanism for the modelled reduction in habitat suitability as discovered in other systems (Morgan *et al.*,

2001; Johansen *et al.*, 2015), particularly in the High Plains and Edwards Plateau regions where warming is projected to increase most. Additional laboratory research could test this hypothesis. Regardless, the message remains that inference into the effects of climate change on fish distributions depends on the methodology used in the assessment and our results point to the potential for unique and perhaps synergistic insights if BEM are integrated to a greater extent.

For Review Only

1
2
3
4
5
6
7
8
9
10
11
12
13
14
15
16
17
18
19
20
21
22
23
24
25
26
27
28
29
30
31
32
33
34
35
36
37
38
39
40
41
42
43
44
45
46
47
48
49
50
51
52
53
54
55
56
57
58
59
60

FUNDING

There is no funding to report.

ACKNOWLEDGEMENTS

n/a

For Review Only

REFERENCES

- Ackerly DD, Loarie SR, Cornwell WK, Weiss SB, Hamilton H, Branciforte R, Kraft NJB (2010) The geography of climate change: implications for conservation biogeography. *Divers Distrib* 16:476-487.
- Anderson RP, Araújo M, Guisan A, Lobo JM, Martínez-Meyer E, Peterson AT, Soberón J (2016) *Final Report of the Task Group on GBIF Data Fitness for Use in Distribution Modelling*.
- Bean PT, Lutz-Carrillo DJ, Bonner TH (2013) Rangewide survey of the introgressive status of Guadalupe Bass: implications for conservation and management. *Trans Am Fish Soc* 142:681-689.
- Birdsong TW, Allen MS, Claussen JE, Garrett GP, Grabowski TB, Graham J, Tringali MD (2015) Native black bass initiative: implementing watershed-scale approaches to conservation of endemic black bass and other native fishes in the southern United States. In: Tringali MD, Long JM, Birdsong TW, Allen MS, eds. Black bass diversity: multidisciplinary science for conservation. American Fisheries Society Symposium, Bethesda pp 363-378.
- Briscoe NJ, Kearney MR, Taylor CA, Wintle BA (2016) Unpacking the mechanisms captured by a correlative species distribution model to improve predictions of climate refugia. *Glob Change Biol* 22:2425-2439.
- Buckley, LB (2008) Linking traits to energetics and population dynamics to predict lizard ranges in changing environments. *Am Nat* 171:E1-E19.
- Buckley LB, Waaser SA, MacLean HJ, Fox R (2011) Does including physiology improve species distribution model predictions of responses to recent climate change? *Ecology* 92:2214-2221.
- Bush AA, Nipperess DA, Duursma DE, Theischinger G, Turak E, Hughes L (2014) Continental-scale assessment of risk to the Australian Odonata from climate change *PLOS ONE*, 9.
- Caldwell TG, Wolaver BD, Bongiovanni T, Pierre JP, Robertson S, Abolt C, Scanlon BR (2020) Spring discharge and thermal regime of a groundwater dependent ecosystem in an arid karst environment. *J Hydrol* 587:124947.
- Comte L, Grenouillet G (2013) Do stream fish track climate change? Assessing distribution shifts in recent decades. *Ecography* 36:1236-1246.
- Chown SL, Gaston KJ (2016) Macrophysiology—progress and prospects. *Funct Ecol* 30:330-344.
- Comte L, Olden JD (2017) Evolutionary and environmental determinants of freshwater fish thermal tolerance and plasticity. *Glob Change Biol* 23:728-736.

- Crossman ND, Brya BA, Summers DM (2012) Identifying priority areas for reducing species vulnerability to climate change. *Divers Distrib* 18:60-72.
- Curtis SG, Perkin JS, Bean PT, Sullivan ML, Bonner TH (2015) Guadalupe Bass *Micropterus treculii* (Vaillant Bocourt, 1874) In: Tringali MD, Long JM, Birdsong TW, Allen MS, eds. Black bass diversity: multidisciplinary science for conservation. American Fisheries Society Symposium, Bethesda pp 55-60.
- Deines AM, Bunnell DB, Rogers MW, Beard TD, Taylor WW (2015) A review of the global relationship among freshwater fish, autotrophic activity, and regional climate. *Rev Fish Biol Fisher* 25:323-336.
- Deslauriers D, Chipps SR, Breck JE, Rice JA, Madenjian CP (2017) Fish bioenergetics 4.0: an R-based modeling application. *Fisheries* 42:586-596.
- Deutsch CA, Tewksbury JJ, Huey RB, Sheldon KS, Ghalambor CK, Haak DC, Martin PR (2008) Impacts of climate warming on terrestrial ectotherms across latitude. *Proc Nat Acad Sci* 105:6668-6672.
- Dillon ME, Wang G, Huey RB (2010) Global metabolic impacts of recent climate warming. *Nature* 467:704-706.
- Edwards RJ (1980) The ecology and geographic variation of the Guadalupe bass, *Micropterus treculii*. Doctoral dissertation. The University of Texas at Austin.
- Elith J, Leathwick JR (2009) Species distribution models: ecological explanation and prediction across space and time. *Annu Rev Ecol Evol Syst* 40:677-697.
- Feeley KJ, Silman MR (2010) Biotic attrition from tropical forests correcting for truncated temperature niches. *Glob Change Biol* 16:1830-1836.
- Fick SE, Hijmans RJ (2017) WorldClim 2: new 1-km spatial resolution climate surfaces for global land areas. *Int J Climatol* 37:4302-4315.
- Finstad AG, Forseth T, Jonsson B, Bellier E, Hesthagen T, Jensen AJ, Hessen DO, Foldvik, A (2011) Competitive exclusion along climate gradients: energy efficiency influences the distribution of two salmonid fishes, *Glob Change Biol* 17:1703-1711.
- Firkus T, Rahel FJ, Bergman HL, Cherrington BD (2018) Warmed winter water temperatures alter reproduction in two fish species. *Environ Manag* 61:291-303.
- Frimpong EA, Huang J, Liang Y (2016) IchthyMaps: A database of historical distributions of freshwater fishes of the United States. *Fisheries* 41:590-599.
- Fullerton AH, Garvey JE, Wright RA, Stein RA (2000) Overwinter growth and survival of largemouth bass: interactions among size, food, origin, and winter severity. *Trans Am Fish Soc* 129:1-12.

- Garvey JE, Wright RA, Stein RA (1998) Overwinter growth and survival of age-0 largemouth bass (*Micropterus salmoides*): revisiting the role of body size. *Can J Fish Aquat Sci* 55:2414-2424.
- Groeschel-Taylor JR, Miyazono S, Grabowski TB, Garrett GP (2019) Growth and habitat use of Guadalupe Bass in the South Llano River, Texas. *J Fish Wildl Manag* 11:33-45.
- Graham CH, Silva N, Velásquez-Tibatá J (2010) Evaluating the potential causes of range limits of birds of the Colombian Andes. *J Biogeog* 37:1863-1875.
- Hanson PC, Johnson TB, Schindler DE, Kitchell JF (1997) *Fish Bioenergetics 3.0*. University of Wisconsin Sea Grant Institute, Madison, Wisconsin.
- Hartman KJ (2017) Bioenergetics of brown bullhead in a changing climate. *Trans Am Fish Soc* 146:634-644.
- Heins DC (2020) Inter-annual variation of exogenous cues influences reproductive phenology of the longnose shiner, *Notropis longirostris*. *Southeast Nat* 19:553-566.
- Henderson MA, Ward FJ (1978) Changes in the chemical composition, calorific and water content of yellow perch fry, *Perca fluviatilis flavescens*. *Verh Internat Verein Limnol* 20:2025-2030.
- Herrera-R GA, Oberdorff T, Anderson EP, Brosse S, Carvajal-Vallejos FM, Frederico RG, Hidalgo M, Jézéquel C, Maldonado M, Maldonado-Ocampo JA *et al.* (2020) The combined effects of climate change and river fragmentation on the distribution of Andean Amazon fishes. *Glob Change Biol* 26:5509-5523.
- Hill RA, Weber MH, Leibowitz SG, Olsen AR, Thornbrugh DJ (2016) The Stream-Catchment (StreamCat) Dataset: A database of watershed metrics for the conterminous United States. *J Am Water Resour As* 52:120-128
- Hoagstrom CW, Brooks JE, Davenport SR (2011) A large-scale conservation perspective considering endemic fishes of the North American plains. *Biol Cons* 144:21-34.
- Hoeinghaus DJ, Winemiller KO, Birnbaum JS (2007) Local and regional determinants of stream fish assemblage structure: inferences based on taxonomic vs functional groups. *J Biogeog* 34:324-338.
- Hollowed AB, Curchitser EN, Stock CA, Zhang CI (2013) Trade-offs associated with different modeling approaches for assessment of fish and shellfish responses to climate change. *Climatic Change* 119:111-129.
- Holt RD, Keitt TH, Lewis MA, Maurer BA, Taper ML (2005) Theoretical models of species' borders: single species approaches. *Oikos* 108:18-27.
- Huang J, Frimpong EA (2015) Using historical atlas data to develop high-resolution distribution models of freshwater fishes. *PLOS ONE* 10.

- Hubbs C, Edwards RJ, Garrett GP (2008) An annotated checklist of the freshwater fishes of Texas, with keys to identification of species. 2nd Edition. *Tex Acad Sci*.
- Isaak DJ, Wenger SJ, Peterson EE, Ver Hoef JM, Nagel DE, Luce CH, Hostetler SW, Dunham JB, Roper BB Wollrab SP *et al.* (2017) The NorWeST summer stream temperature model and scenarios for the western US: A crowd-sourced database and new geospatial tools foster a user community and predict broad climate warming of rivers and streams. *Water Resour Res* 53:9181-9205.
- Jackson DA, Peres-Neto PR, Olden JD (2001) What controls who is where in freshwater fish communities the roles of biotic, abiotic, and spatial factors. *Can J Fish Aquat Sci* 58:157-170.
- Jankowski JE, Robinson SK, Levey DJ (2010) Squeezed at the top: Interspecific aggression may constrain elevational ranges in tropical birds. *Ecology* 91:1877-1884.
- Jelks HL, Walsh SJ, Burkhead NM, Contreras-Balderas S, Diaz-Pardo E, Hendrickson DA, Lyons J, Mandrak NE, McCormick F, Nelson JS *et al.* (2008) Conservation status of imperiled North American freshwater and diadromous fishes. *Fisheries* 33:372-407.
- Jiménez-Valverde A, Nakazawa Y, Lira-Noriega A, Peterson AT (2009) Environmental correlation structure and ecological niche model projections. *Biodiversity Informatics*, 6:28-35.
- Johansen JL, Pratchett MS, Messmer V, Coker DJ, Tobin AJ, Hoey AS (2015) Large predatory coral trout species unlikely to meet increasing energetic demands in a warming ocean. *Scientific Reports* 5:1-8.
- Kearney M, Phillips BL, Tracy CR, Christian KA, Betts G, Porter WP (2008) Modelling species distributions without using species distributions: the cane toad in Australia under current and future climates. *Ecography* 31:423-434.
- Kearney M, Porter WP (2009) Mechanistic niche modelling: combining physiological and spatial data to predict species' ranges. *Ecology Letters* 12:334-350.
- Kitchell JF, Stewart DJ, Weininger D (1977) Applications of a bioenergetics model to yellow perch (*Perca flavescens*) and walleye (*Stizostedion vitreum vitreum*). *J Fish Board Can* 34:1922-1935.
- Lawrence DJ, Beauchamp DA, Olden JD (2015) Life-stage-specific physiology defines invasion extent of a riverine fish. *J Anim Ecol* 84:879-888.
- Mateo RG, Croat TB, Felicísimo ÁM, Muñoz J (2010) Profile or group discriminative techniques? Generating reliable species distribution models using pseudo-absences and target-group absences from natural history collections. *Divers Distrib* 16:84-94.

- McGarvey DJ, Menon M, Woods T, Tassone S, Reese J, Vergamini M, Kellogg E (2018) On the use of climate covariates in aquatic species distribution models: are we at risk of throwing out the baby with the bath water? *Ecography* 41:695-712.
- McManamay RA, Utz RM (2014) Open-access databases as unprecedented resources and drivers of cultural change in fisheries science. *Fisheries* 39:417-425.
- Morgan IJ, McDonald DG, Wood CM (2001) The cost of living for freshwater fish in a warmer, more polluted world. *Glob Change Biol* 7:345-355.
- Muneepeerakul R, Bertuzzo E, Lynch HJ, Fagan WF, Rinaldo A, Rodriguez-Iturbe I (2008) Neutral metacommunity models predict fish diversity patterns in Mississippi–Missouri basin. *Nature*, 453:220-222.
- Nagel D, Wollrab S, Parkes-Payne S, Peterson E, Isaak D, Ver Hoef J (2017) National Stream Internet Hydrography Datasets for Spatial-Stream-Network (SSN) Analysis. Rocky Mountain Research Station: Fort Collins, CO, USA.
- NatureServe (2010) *Digital Distribution Maps of the Freshwater Fishes in the Conterminous United States*. Version 3.0. Arlington, VA U.S.A.
- Near TJ, Kassler TW, Koppelman JB, Dillman CB, Philipp DP (2003) Speciation in North American black basses, *Micropterus* (Actinopterygii: Centrarchidae) *Evolution* 57:1610-1621.
- Patrick CJ, McGarvey DJ, Larson JH, Cross WF, Allen DC, Benke AC, Brey T, Huryn AD, Jones J, Murphy CA (2019) Precipitation and temperature drive continental-scale patterns in stream invertebrate production. *Science Advances* 5. doi.org/10.1126/sciadv.aav2348
- Pease AA, Paukert CP (2014) Potential impacts of climate change on growth and prey consumption of stream-dwelling smallmouth bass in the central United States. *Ecol Freshw Fish* 23:336-346.
- Perkin JS, Shattuck ZR, Bean PT, Bonner TH, Saraeva E, Hardy TB (2010) Movement and microhabitat associations of Guadalupe Bass in two Texas rivers. *N Am J Fish Manage* 30:33-46.
- Perkin JS, Gido KB, Cooper AR, Turner TF, Osborne MJ, Johnson ER, Mayes KB (2015) Fragmentation and dewatering transform Great Plains stream fish communities. *Ecol Monogr* 85:73-92.
- Petersen JH, DeAngelis DL, Paukert CP (2008) An overview of methods for developing bioenergetic and life history models for rare and endangered species. *Trans Am Fish Soc* 137:244-253.
- Phillips SJ, Dudík M, Schapire RE (2004) A maximum entropy approach to species distribution modeling. Proceedings of the twenty-first international conference on machine learning. doi.org/10.1145/1015330.1015412

- Punzet M, Voß F, Voß A, Kynast E, Bärlund I (2012) A global approach to assess the potential impact of climate change on stream water temperatures and related in-stream first-order decay rates. *J Hydrometeorol* 13:1052-1065.
- Radinger J, Hölker F, Horký P, Slavík O, Dendoncker N, Wolter C (2016) Synergistic and antagonistic interactions of future land use and climate change on river fish assemblages. *Glob Change Biol* 22:1505-1522.
- Rypel AL (2014) Do invasive freshwater fish species grow better when they are invasive? *Oikos* 123:279-289.
- Sax DF, Early R, Bellemare J (2013) Niche syndromes, species extinction risks, and management under climate change. *Trends Ecol Evol* 28:517-523.
- Shuter BJ, Finstad AG, Helland IP, Zweimüller I, Hölker F (2012) The role of winter phenology in shaping the ecology of freshwater fish and their sensitivities to climate change. *Aquat Sci* 74:637-657.
- Smith VB, David CH, Cardenas MB, Yang ZL (2013) Climate, river network, and vegetation cover relationships across a climate gradient and their potential for predicting effects of decadal-scale climate change. *J Hydrol* 488:101-109.
- Soberón J (2007) Grinnellian and Eltonian niches and geographic distributions of species. *Ecol Lett* 10:1115-1123.
- Strayer DL, Dudgeon D (2010) Freshwater biodiversity conservation: recent progress and future challenges. *J N Am Benthol Soc* 29:344-358.
- Sullivan ML, Zhang Y, Bonner TH, Tomasso JR (2013) Temperature modulation of growth and physiology of juvenile Guadalupe Bass. *N Am J Aquacult* 75:373-376.
- Sunday JM, Bates AE, Dulvy NK (2011) Global analysis of thermal tolerance and latitude in ectotherms. *Proc Roy Soc B Biol Sci* 278:1823-1830.
- Taniguchi Y, Nakano S (2000) Condition-specific competition: implications for the altitudinal distribution of stream fishes. *Ecology* 81:2027-2039.
- Thomas ZA (2015) Fishing warmwater streams with limited public access: angling behavior, economic impact, and the role of Guadalupe Bass in a twenty-four county region of Texas. Masters thesis. Texas Tech University.
- Tonn WM, Magnuson JJ, Rask M, Toivonen J (1990) Intercontinental comparison of small-lake fish assemblages: the balance between local and regional processes. *Am Nat* 136:345-375.
- Troia MJ, Kaz AL, Niemeyer JC, Giam X (2019) Species traits and reduced habitat suitability limit efficacy of climate change refugia in streams. *Nat Ecol Evol* 3:1321-1330.

- Urban MC, Tewksbury JJ, Sheldon KS (2012) On a collision course: competition and dispersal differences create no-analogue communities and cause extinctions during climate change. *Proc Roy Soc B Biol Sci* 279:2072-2080.
- Vörösmarty CJ, McIntyre PB, Gessner MO, Dudgeon D, Prusevich A, Green P, Glidden S, Bunn SE, Sullivan CA, Reidy Liermann C (2010) Global threats to human water security and river biodiversity. *Nature* 467:555-561.
- Vollering J, Halvorsen R, Mazzoni S (2019) The MIAMaxent R package: Variable transformation and model selection for species distribution models. *Ecol Evol* 9:12051-12068.
- Wang T, Hamann A, Spittlehouse D, Carroll C (2016) Locally downscaled and spatially customizable climate data for historical and future periods for North America *PLOS ONE* 11.
- Wood SN, Scheipl F (2014) gamm4: generalized additive mixed models using mgcv and lme4. Version 0.2-2. R package.
- Wood ZT, Shepard ID, Hurley ST, Paisker MR, Hensley VR, Kinnison MT (2020) Sex-Dependent Cold Tolerance at the Northern Invasive Range Limit of *Gambusia affinis* on Cape Cod, Massachusetts. *Copeia* 108:670-678.

Table 1. Summary of species distribution modeling (SDM) projection conditions and results.

Projection	Projection conditions				Projection results				
	Time period	Emissions scenario	Δ T	Δ P	Occupancy*	Colonize	Extirpate	Persist	Unoccupied
1	1960-1990	Historical	n/a	n/a	2,821	n/a	n/a	n/a	n/a
2	2071-2100	RCP 4.5	✓	✓	-33.9	92	1,065	1,806	4,910
3	2071-2100	RCP 4.5	✓		-26.0	88	835	2,036	4,914
4	2071-2100	RCP 4.5		✓	-7.6	158	375	2,496	4,844
5	2071-2100	RCP 8.5	✓	✓	-44.1	230	1,496	1,375	4,772
6	2071-2100	RCP 8.5	✓		-34.7	229	1,226	1,645	4,773
7	2071-2100	RCP 8.5		✓	-4.6	117	249	2,622	4,885

* Projection 1 is the number of reaches occupied. Projections 2-7 are the percent changes in number of reaches occupied between historical and future time periods.

Figure 1. Distribution of Guadalupe bass in central Texas. (A) Distribution of IchthyMaps occurrence records, (B) SDM-projected habitat suitability, and SDM-projected occupancy transitions between historical and future climate scenarios assuming (C) moderate and (D) high emissions scenarios. Pie charts show proportion of 8,119 reaches in each occupancy transition and the yellow square denoting the South Llano River is the location from which growth data were obtained. Panels (C) and (D) illustrate projections 2 and 5 from Table 1, respectively.

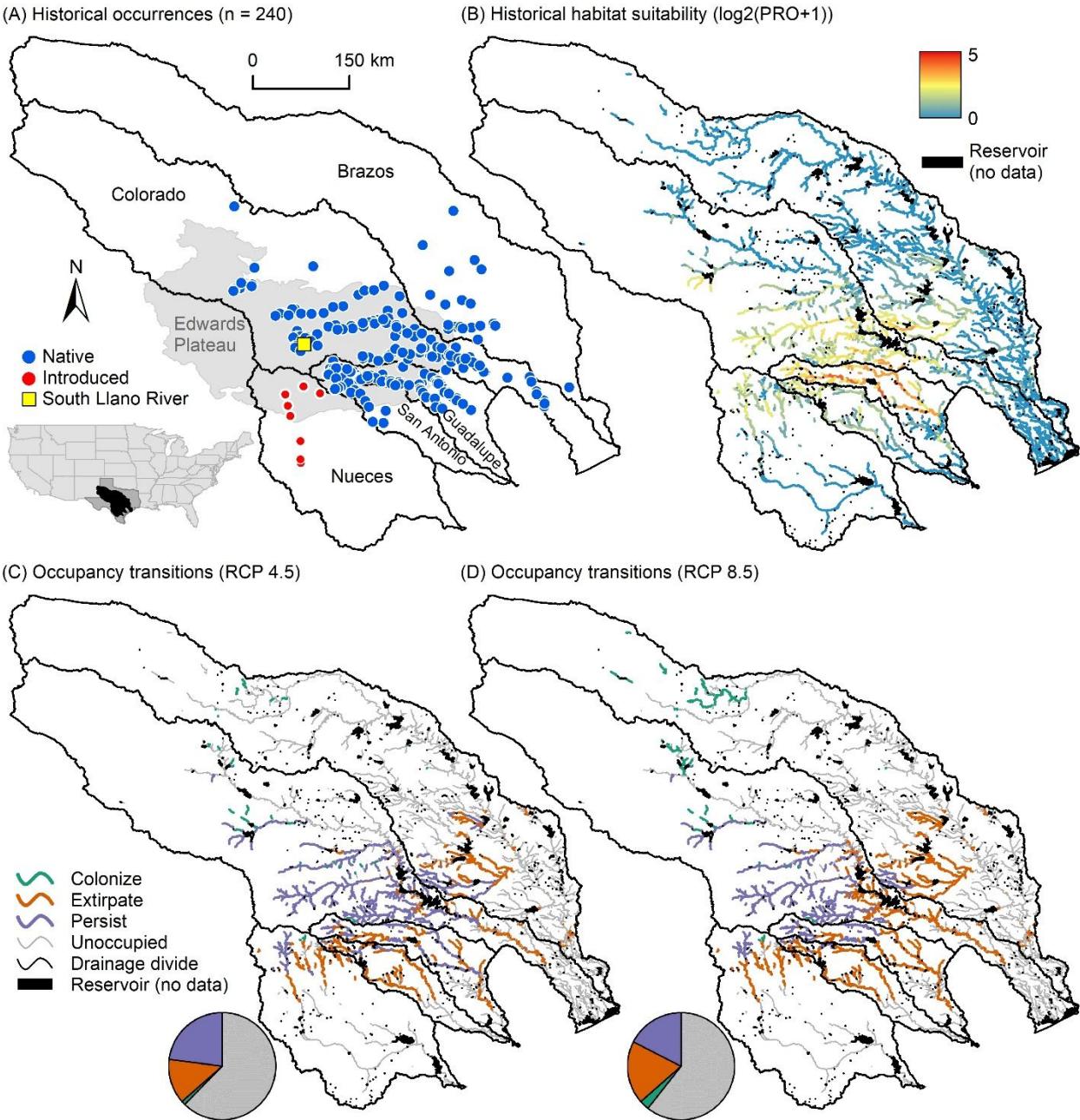


Figure 2. Empirical validation of Guadalupe Bass bioenergetics modelling. Relationship between Julian day and simulated growth of age-1 Guadalupe bass in the South Llano River from 2006-2011. Each solid line represents one of 500 simulations (50 synthetic parameter sets x 5 C_p scenarios x 2 R_{ACT} scenarios). Colored red or blue lines ($n = 36$) represent simulated growth trajectories within $\pm 2.5\%$ of end-of-year empirical length (green dashed lines). Blue and red lines represent $R_{ACT} = 1.0$ and $R_{ACT} = 1.5$ scenarios, respectively.

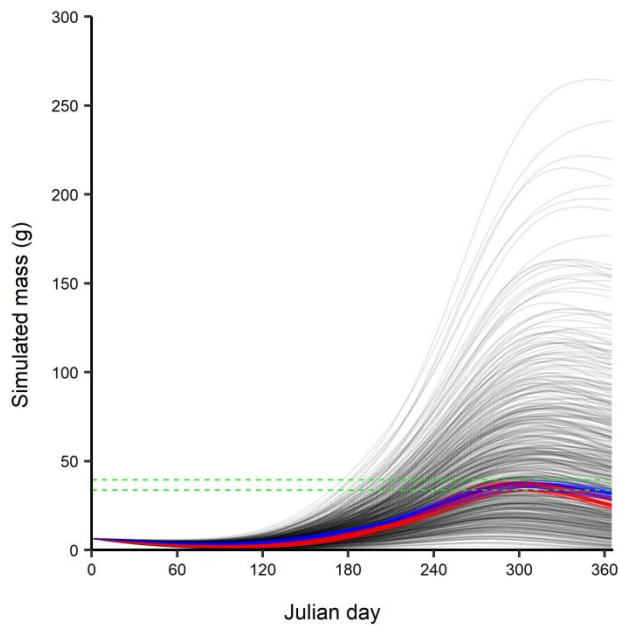


Figure 3. Bioenergetic model-projected performance. (A) Ensemble mean and (B) uncertainty in BEM-projected growth of age-1 Guadalupe bass under historical climate for 8,119 reaches within the Guadalupe bass range. Change in growth of age-1 Guadalupe bass between historical and future climate scenarios assuming (C) moderate and (D) high emissions scenarios.

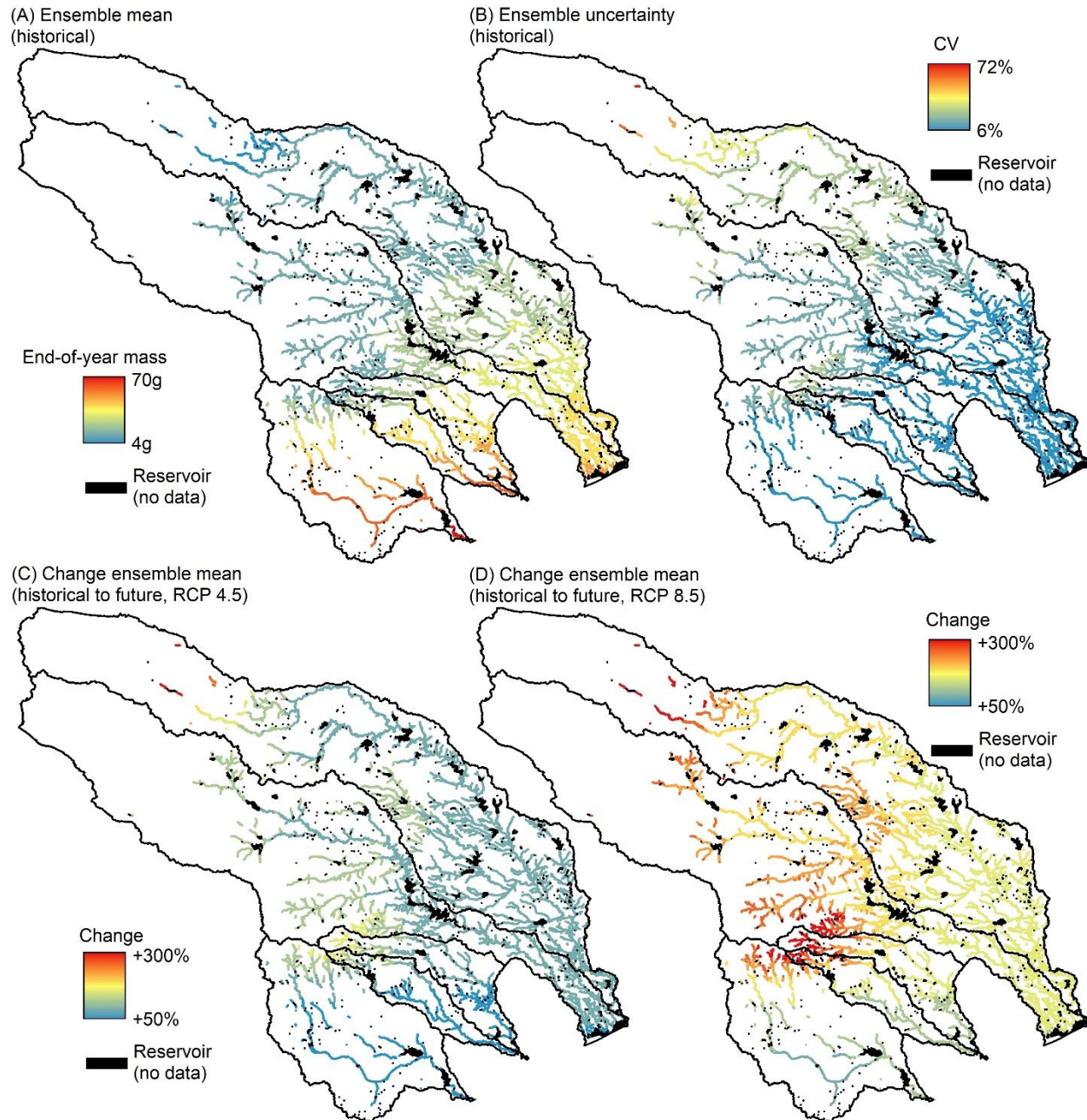


Figure 4. Seasonal variation in bioenergetics. Relationship between Julian day and (A-C) simulated daily growth of age-1 or (D-F) simulated cumulative growth of age-1 Guadalupe bass averaged across 2,871 historically-occupied reaches under (A,D) historical and (B-C, E-F) future climate scenarios. Each solid line represents a simulation from one of 36 empirically-validated parameter sets.

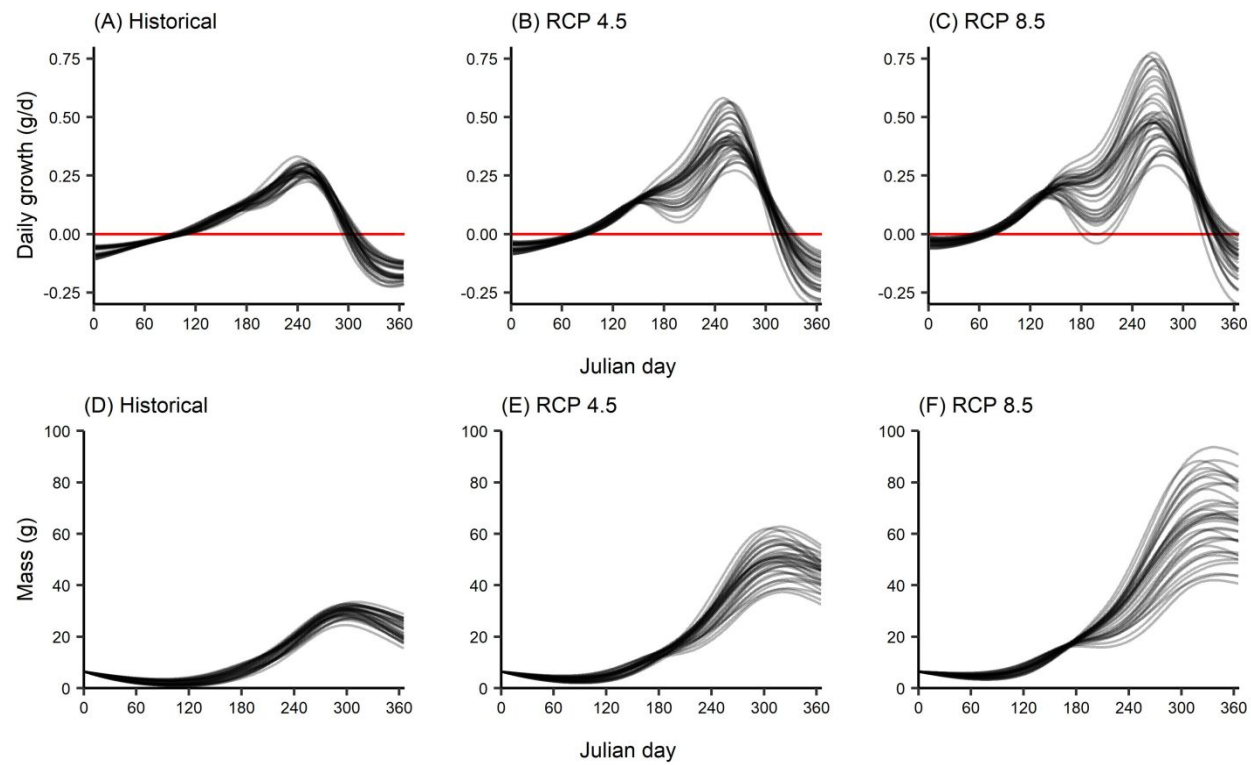


Figure 5. Historical concordance between BEMs and SDMs. Relationship between BEM-projected end-of-year mass and ENM-projected habitat suitability for the historical time period. Lines represent GAM fits for (A) all inter-confluence stream reaches and (B) each of three regions: High Plains (blue), Edwards Plateau (green), and Coastal Plain (red).

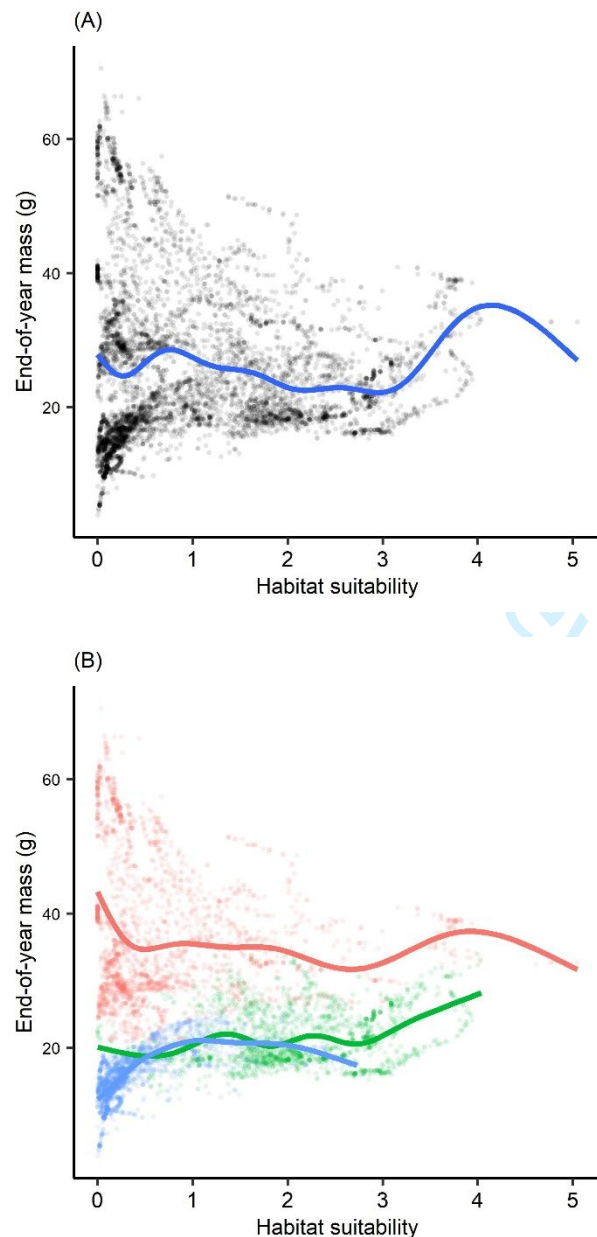
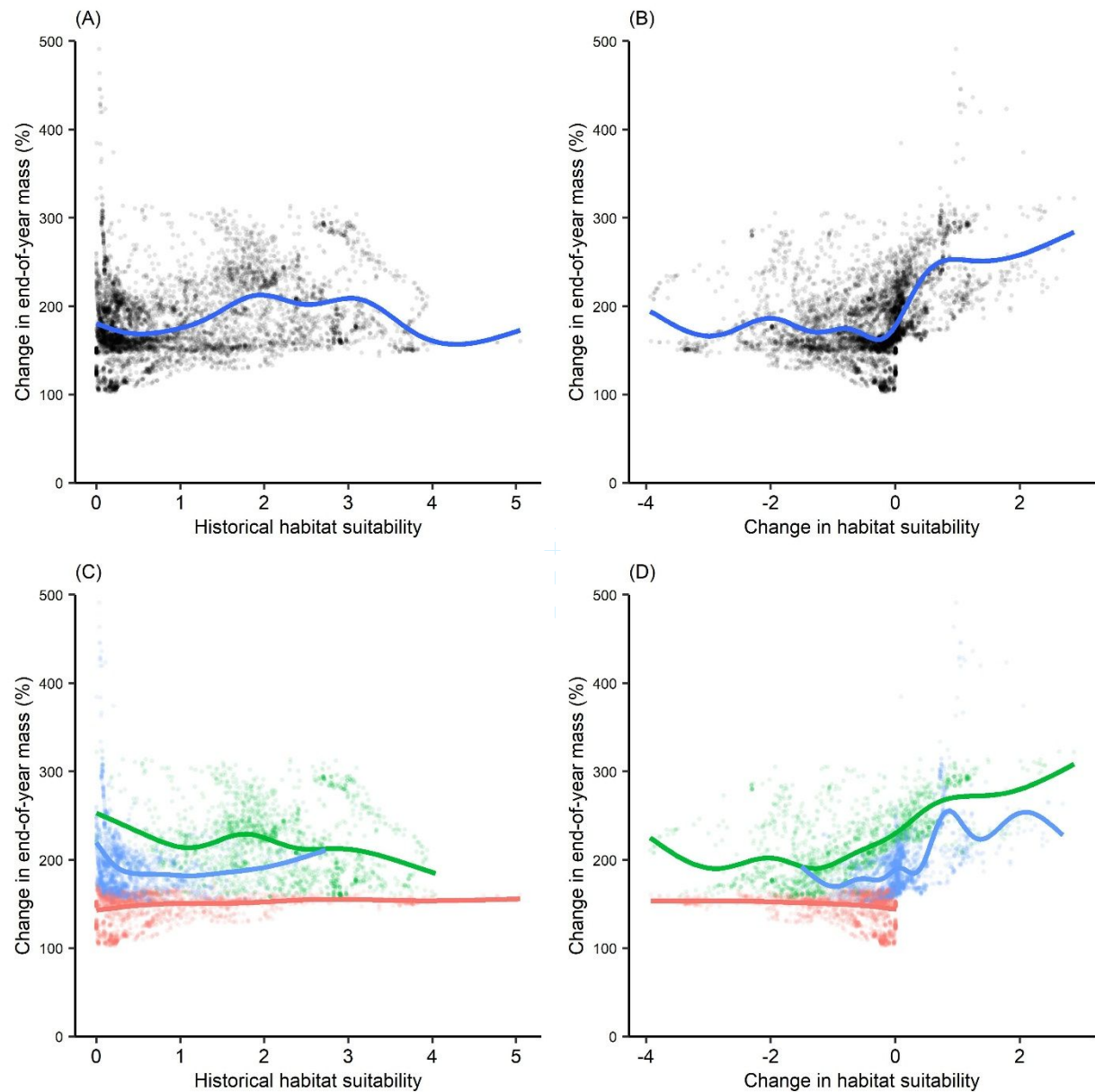


Figure 6. Future concordance between BEMs and SDMs. (A, C) Relationship between historical-to-future change in end-of-year mass and historical habitat suitability. (B, D) Relationship between historical-to-future change in end-of-year mass and historical-to-future change in habitat suitability. Lines represent GAM fits for (A-B) all inter-confluence stream reaches and (C-D) each of three regions: High Plains (blue), Edwards Plateau (green), and Coastal Plain (red).



Supplementary Table 1. Environmental covariates used for species distribution models.

Covariate	Description	Range	Units	Source	Importance*
TotDASqKM	Catchment area	0 – 207526.3	km ²	NHD	0.00
SLOPE	Reach slope	0.0001 – 2.17	%	NHD	0.00
BFI	Baseflow index	2 – 61.48213	%	StreamCat	-2.01
HydrlCond	Lithological hydraulic conductivity	0.000004 – 224.6375	µm·sec ⁻¹	StreamCat	-0.37
CompStrgth	Lithological uniaxial compressive strength	0.333 – 188.6766	megaPascals	StreamCat	-0.51
Kffact	Soil erodibility (Kf) factor	0 – 0.4542416	unitless	StreamCat	-1.09
Runoff	Runoff	0 – 406.6479	mm	StreamCat	0.97
Perm	Permeability of soils	0.44 – 23.43	cm·h ⁻¹	StreamCat	-0.33
RckDep	Depth to bedrock of soils	30.79 – 152.4	cm	StreamCat	0.07
WtDep	Seasonal water table depth of soils	31.044918 – 183.9073	cm	StreamCat	-0.24
WetIndex	Composite Topographic Index	572.475096 – 1765.25	unitless	StreamCat	-0.13
PctCarbRes	Lithology: carbonate residual material	0 – 100	%	StreamCat	0.10
PctNonCarb	Lithology: non-carbonate residual material	0 – 100	%	StreamCat	0.39
PctSilicic	Lithology: silicic residual material	0 – 100	%	StreamCat	0.04
PctEolCrs	Lithology: eolian coarse sediment	0 – 100	%	StreamCat	0.36
PctEolFine	Lithology: eolian fine sediment	0 – 5.048054	%	StreamCat	0.01
PctSalLake	Lithology: saline lake sediment	0 – 4.316827	%	StreamCat	0.00
PctAlluvCo	Lithology: coarse alluvium	0 – 100	%	StreamCat	0.42
Tmax07	Max. temp. in the warmest month	31.9 – 37.4	°C	ClimateNA	0.06
Tmin01	Min. temp. in the coldest month	-6.7 – 7.4	°C	ClimateNA	-1.13
PPT05	Prec. in the wettest month	43 – 143	mm	ClimateNA	0.10
PPT10	Prec. in the driest month	30 – 129	mm	ClimateNA	0.74
PPT07	Prec. in the warmest month	30 – 114	mm	ClimateNA	-0.16
PPT01	Prec. in the coldest month	9 – 99	mm	ClimateNA	0.62

* Percent change in AUC with the covariate withheld from the model. Value represents mean of 10 independent cross validations.

Supplementary Table 2. Parameter set for largemouth bass and for 36 synthetic parameter sets used to project Guadalupe bass growth.

Parameter set	C _P	C _A	C _B	CTM	CTO	C _Q	R _{ACT}	R _A	R _B	R _Q	F _A	U _A	SDA	ED
(LMB) ^A	0.50	0.3300	-0.3250	37.0	27.5	2.65	1.0	0.0084	-0.3550	0.0313	0.1040	0.0882	0.1600	4184
Set_20	0.73	0.3345	-0.3349	36.1	28.8	2.71	1.5	0.0083	-0.3455	0.0304	0.1011	0.0899	0.1551	4098
Set_38	0.67	0.3317	-0.3201	36.0	28.3	2.54	1.5	0.0080	-0.3540	0.0320	0.1042	0.0917	0.1632	4312
Set_52	0.47	0.3304	-0.3091	36.3	27.6	2.67	1.0	0.0081	-0.3379	0.0311	0.1084	0.0924	0.1580	4174
Set_72	0.47	0.3276	-0.3330	38.2	26.6	2.65	1.0	0.0084	-0.3702	0.0328	0.1067	0.0867	0.1622	4284
Set_83	0.50	0.3295	-0.3189	38.4	28.3	2.61	1.0	0.0086	-0.3611	0.0324	0.1071	0.0844	0.1560	4119
Set_89	0.70	0.3295	-0.3189	38.4	28.3	2.61	1.5	0.0086	-0.3611	0.0324	0.1071	0.0844	0.1560	4119
Set_108	0.67	0.3429	-0.3378	36.3	27.3	2.69	1.5	0.0083	-0.3473	0.0324	0.1051	0.0867	0.1594	4211
Set_117	0.64	0.3189	-0.3203	37.3	26.1	2.72	1.5	0.0083	-0.3458	0.0319	0.1027	0.0870	0.1542	4074
Set_168	0.67	0.3252	-0.3267	38.3	27.8	2.66	1.5	0.0083	-0.3613	0.0314	0.1009	0.0885	0.1582	4179
Set_183	0.50	0.3416	-0.3367	37.8	27.9	2.77	1.0	0.0083	-0.3625	0.0327	0.1040	0.0880	0.1611	4254
Set_203	0.50	0.3251	-0.3151	38.7	28.5	2.53	1.0	0.0085	-0.3553	0.0316	0.0998	0.0841	0.1656	4373
Set_209	0.70	0.3251	-0.3151	38.7	28.5	2.53	1.5	0.0085	-0.3553	0.0316	0.0998	0.0841	0.1656	4373
Set_212	0.47	0.3273	-0.3155	38.2	27.8	2.55	1.0	0.0087	-0.3717	0.0306	0.1045	0.0877	0.1614	4263
Set_223	0.50	0.3339	-0.3296	37.2	28.2	2.73	1.0	0.0086	-0.3571	0.0302	0.1063	0.0846	0.1584	4183
Set_229	0.70	0.3339	-0.3296	37.2	28.2	2.73	1.5	0.0086	-0.3571	0.0302	0.1063	0.0846	0.1584	4183
Set_240	0.73	0.3363	-0.3394	36.7	28.3	2.76	1.5	0.0087	-0.3700	0.0322	0.1002	0.0851	0.1576	4163
Set_242	0.47	0.3382	-0.3229	36.0	28.6	2.54	1.0	0.0085	-0.3633	0.0309	0.1011	0.0863	0.1550	4094
Set_248	0.67	0.3382	-0.3229	36.0	28.6	2.54	1.5	0.0085	-0.3633	0.0309	0.1011	0.0863	0.1550	4094
Set_251	0.44	0.3339	-0.3198	37.6	26.4	2.70	1.0	0.0084	-0.3703	0.0323	0.1060	0.0864	0.1634	4317
Set_280	0.73	0.3308	-0.3364	38.8	27.7	2.63	1.5	0.0084	-0.3375	0.0325	0.1050	0.0890	0.1630	4307
Set_282	0.47	0.3362	-0.3111	38.0	28.7	2.57	1.0	0.0086	-0.3705	0.0301	0.1054	0.0885	0.1595	4213
Set_298	0.67	0.3161	-0.3258	36.9	26.7	2.60	1.5	0.0083	-0.3488	0.0322	0.0993	0.0859	0.1573	4154
Set_302	0.47	0.3403	-0.3250	35.3	27.4	2.75	1.0	0.0083	-0.3610	0.0317	0.1021	0.0910	0.1639	4330
Set_317	0.64	0.3180	-0.3329	38.4	26.2	2.65	1.5	0.0085	-0.3569	0.0306	0.1013	0.0868	0.1580	4173
Set_327	0.64	0.3455	-0.3253	37.8	28.3	2.56	1.5	0.0082	-0.3431	0.0307	0.1026	0.0858	0.1587	4191
Set_353	0.50	0.3176	-0.3199	36.8	26.8	2.71	1.0	0.0086	-0.3559	0.0323	0.1010	0.0873	0.1663	4394
Set_359	0.70	0.3176	-0.3199	36.8	26.8	2.71	1.5	0.0086	-0.3559	0.0323	0.1010	0.0873	0.1663	4394
Set_380	0.73	0.3290	-0.3245	38.4	28.1	2.65	1.5	0.0085	-0.3404	0.0327	0.1053	0.0871	0.1545	4081
Set_383	0.50	0.3419	-0.3314	38.4	28.2	2.70	1.0	0.0081	-0.3496	0.0326	0.1061	0.0851	0.1630	4305
Set_392	0.47	0.3338	-0.3165	36.4	28.3	2.64	1.0	0.0081	-0.3636	0.0303	0.1089	0.0849	0.1652	4364
Set_410	0.73	0.3169	-0.3115	35.3	28.2	2.54	1.5	0.0087	-0.3517	0.0322	0.1037	0.0900	0.1550	4093

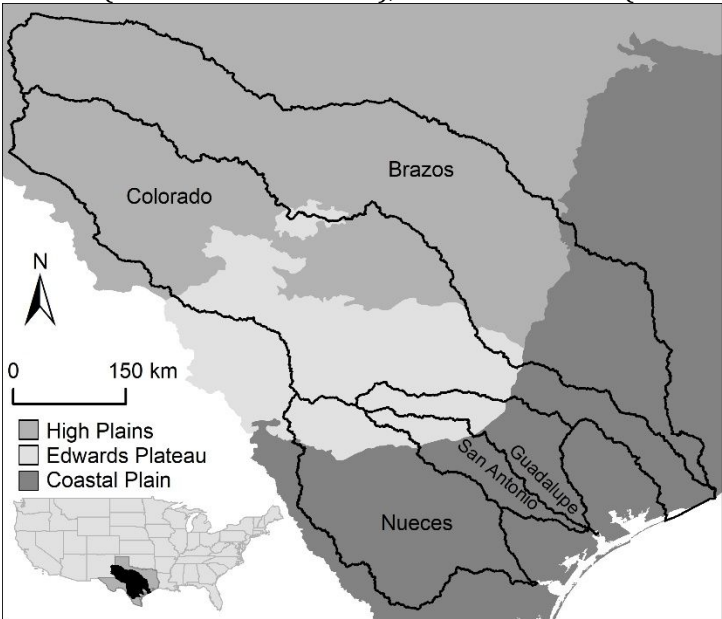
Set_421	0.44	0.3274	-0.3113	36.5	26.8	2.75	1.0	0.0081	-0.3570	0.0306	0.1016	0.0888	0.1611	4255
Set_426	0.61	0.3274	-0.3113	36.5	26.8	2.75	1.5	0.0081	-0.3570	0.0306	0.1016	0.0888	0.1611	4255
Set_442	0.47	0.3318	-0.3301	36.7	26.8	2.58	1.0	0.0084	-0.3456	0.0322	0.0993	0.0887	0.1663	4393
Set_458	0.67	0.3205	-0.3273	38.0	26.8	2.65	1.5	0.0085	-0.3573	0.0322	0.0996	0.0863	0.1617	4270
Set_464	0.53	0.3264	-0.3305	38.6	28.7	2.58	1.0	0.0087	-0.3499	0.0301	0.1029	0.0925	0.1607	4245

^A Largemouth bass from Rice et al. 1983

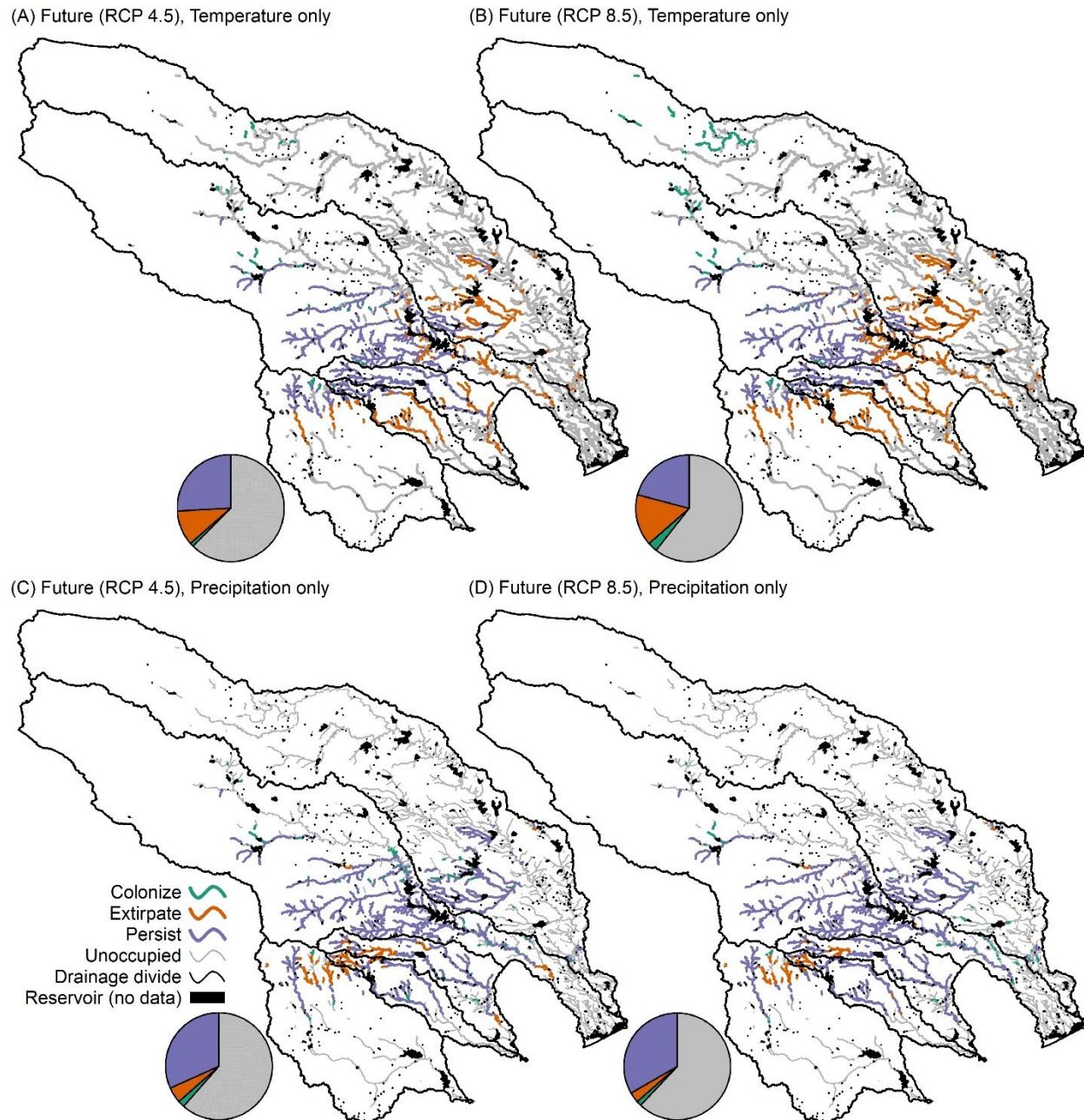
For Review Only

SUPPLEMENTARY MATERIAL

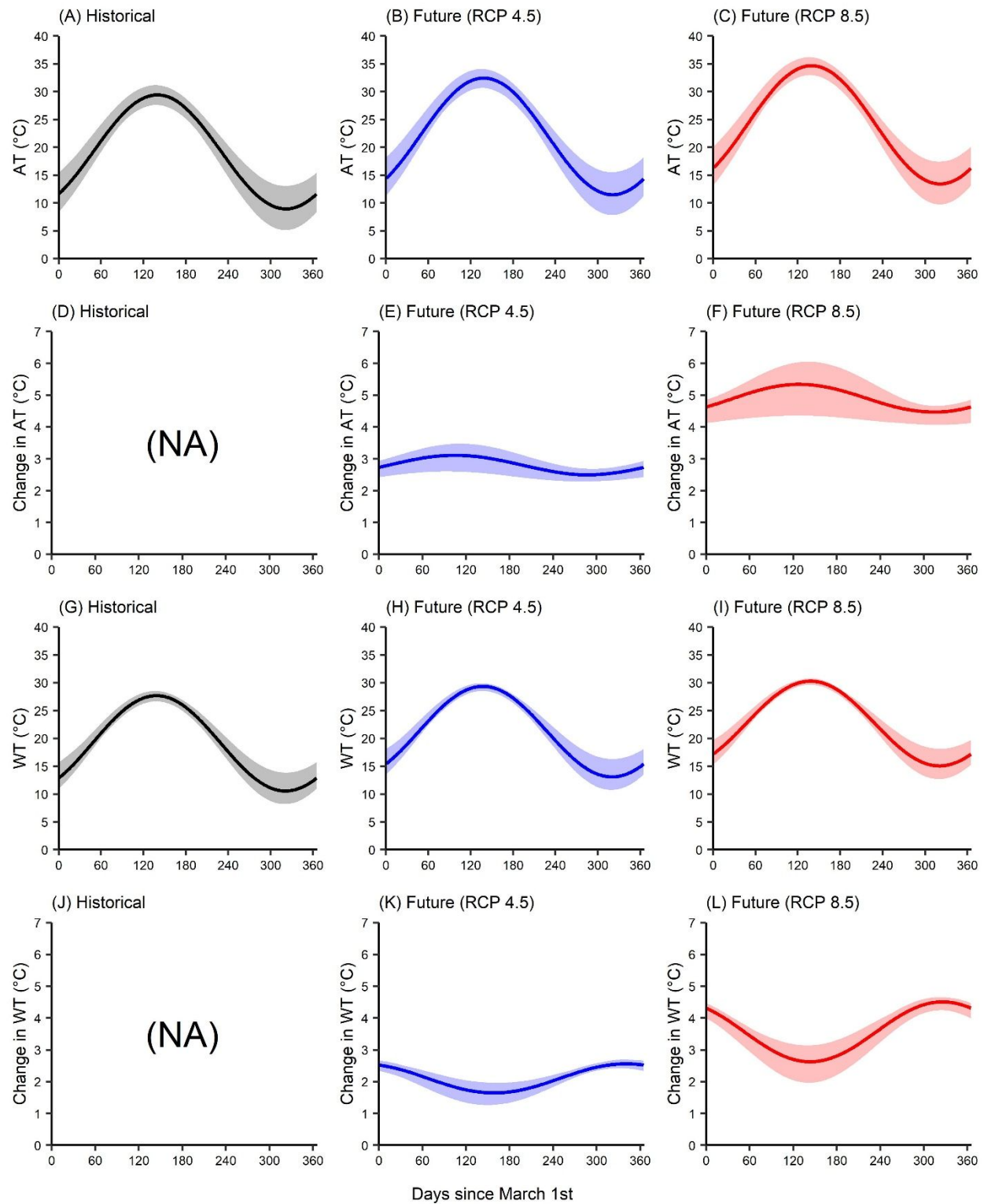
Supplementary Figure 1. Delineation of High Plains (EPA Level III codes 25, 26, 27, 29), Edwards Plateau (EPA Level III code 30), and Coastal Plain (EPA Level III codes 31, 32, 33, 34, 35) regions.



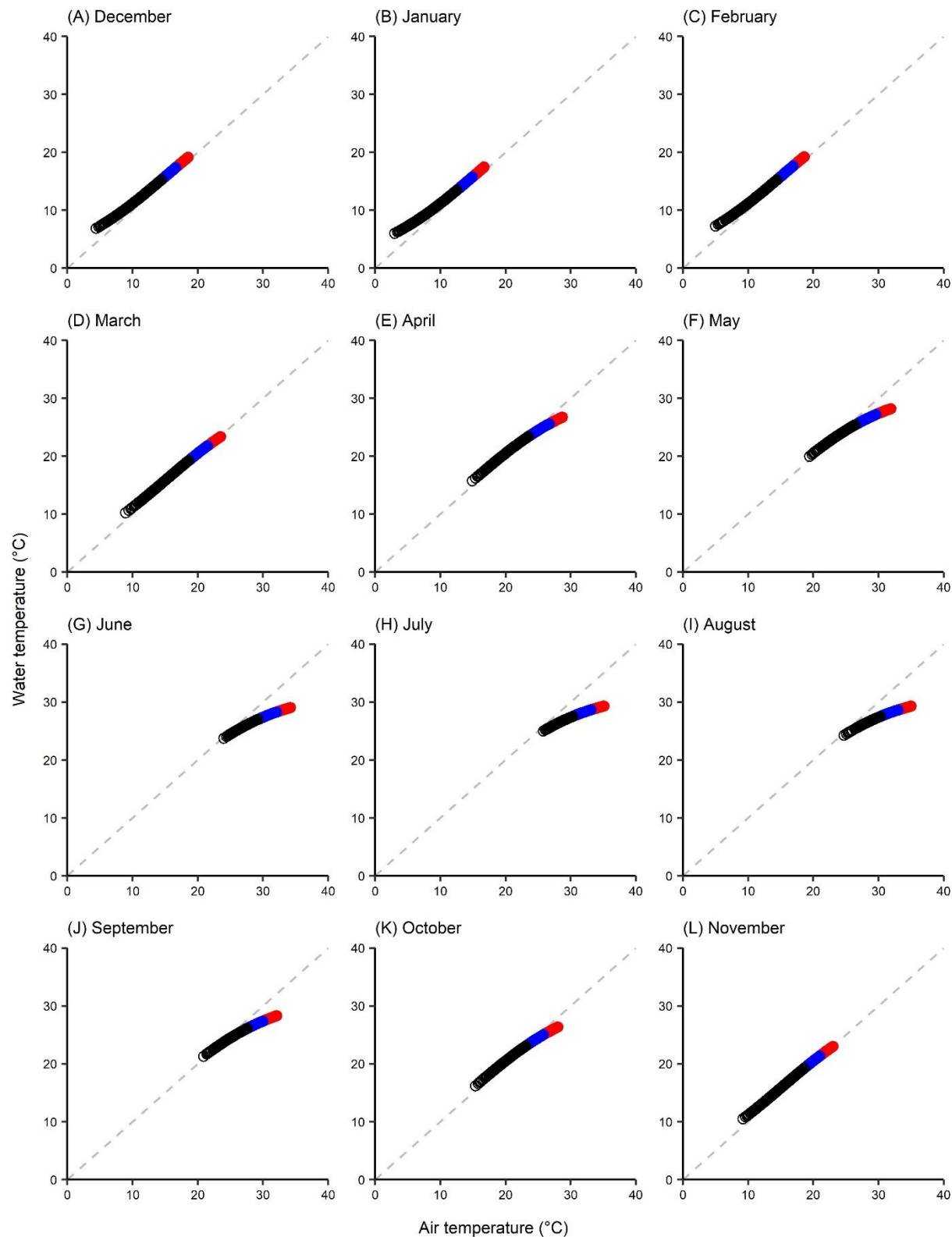
Supplementary Figure 2. SDM-projected occupancy transitions between historical and future climate scenarios assuming (A,C) moderate and (B,D) high emissions scenarios. Projections assume (A-B) altered temperature only and (C-D) altered precipitation only. Panels A, B, C, and D correspond to projections 3, 6, 4, and 7, respectively, from Table 1. See Figure 1 for altered temperature and precipitation. Pie charts show proportion of 8,119 reaches in each occupancy transition. Panels (A), (B), (C), and (D) illustrate projections 3, 6, 4, and 7 from Table 1, respectively.



Supplementary Figure 3. Relationships between mean daily air and water temperature and days since March 1st under historical and future climate scenarios. Daily temperature (air temperature = AT, water temperature = WT) values are interpolated from mean monthly temperatures. Solid lines are the median values across 8,119 reaches and confidence bands span the minima and maxima.



Supplementary Figure 4. Sigmoidal air-water temperature relationships for the warm-temperate Köppen–Geiger climate zone. Each point is the temperature of a reach ($n = 8,119$) under historical climate (black) and future climate assuming moderate (blue) and high (red) emissions.



Supplementary Figure 5. Relationships between (A) respiration and temperature, (B) respiration and mass, (C) consumption and temperature, and (D) consumption and mass. Each line represents one of 500 simulations (50 synthetic parameter sets x 5 C_p scenarios x 2 R_{ACT} scenarios).

